The Astronomical Journal, 136:1964–1979, 2008 November doi:10.1088/0004-6256/136/5/1964

A MODEL FOR THE CHROMOSPHERE/WIND OF 31 CYGNI AND ITS IMPLICATIONS FOR SINGLE STARS

Joel A. Eaton
Center of Excellence in Information Systems, Tennessee State University, Nashville, TN, USA; eaton@donne.tsuniv.edu
Received 2008 March 4; accepted 2008 August 29; published 2008 October 9

ABSTRACT

I develop a detailed empirical model for the chromosphere and wind of 31 Cyg based on a previously published analysis of *International Ultraviolet Explorer* spectra from the 1993 eclipse and on the thermodynamics of how the wind must be driven. I then use this model to interpret observations of single supergiant stars and to assess the evidence that their winds are fundamentally different from those of supergiants in binary systems. This model naturally predicts a certain level of clumping of the gas to balance the pressure that drives the wind. It also predicts that anisotropic turbulence, such as would result from transverse displacements of Alfven waves directed along radial magnetic flux lines, would not give the roughly Gaussian profiles of emission lines seen in cool giant stars. Furthermore, it implies that C II] may not tell us much at all about general conditions in chromospheres. Finally, I speculate that chaotic magnetic fields, in dynamical equilibrium with the gas of the wind, are the actual driving mechanism.

Key words: stars: chromospheres – stars: winds, outflows

1. INTRODUCTION

It is no great stretch to assume that all cool stars (later than mid-F spectral type) have chromospheres and, likely, winds as well. These are regions above the photosphere too hot to be heated radiatively; rather, they must be heated by magnetic processes or by shocks. Most analyses of such stars' chromospheres and winds are based on interpreting the strengths and shapes of emission lines in their spectra. The Sun is the only one for which we can actually map out the chromosphere in any appreciable spatial detail. All the others are unresolved, which limits us to interpreting global properties of the emitting gas in terms of models without any real spatial information (zero dimensional). There are a number of standard diagnostics used in this work. For cool giant and supergiant stars, we have the C II] intersystem multiplet at 2325 Å (Stencel et al. 1981), the Al II] multiplet at 2669 Å (e.g., Judge 1986a, 1986b; Harper 1992), the Mg II *h* and *k* lines (e.g., Stencel et al. 1980; Milkey et al. 1975), an abundance of Fe II lines in the UV (ultraviolet) affected by scattering in winds (Judge & Jordan 1991), Hα (Johnson & Klinglesmith 1965; Mallik 1993), and the H I Lyman lines (Landsman & Simon 1993; Haisch et al. 1977). Many of the lines involved fall in the UV because of the temperatures and densities prevailing in these chromospheres, so our knowledge of cool giants' chromospheres necessarily has developed through observations from the *International Ultraviolet Explorer* (*IUE*) satellite (e.g., Judge 1988) and more recently the *Hubble Space Telescope* (*HST*; e.g., Carpenter et al. 1991, 1995, 1997, 1999). Other observations of these chromospheres involve measuring radio thermal emission from their winds (Drake & Linsky 1986; Harper et al. 2001).

An alternative, complementary approach to mapping the properties of chromospheres solely by interpreting observations of the emission lines of single stars is to use the ζ Aurigae binaries (Wright 1959, 1970; Wilson & Abt 1954) to probe their chromospheres and winds in greater spatial detail (legitimately at least one-dimensionally). These systems consist of a cool supergiant paired with a B dwarf, the prototype system ζ Aur consisting of K4 Ib and B5 V components. Absorptions in the spectrum of the B star by the gas in the wind and chromosphere of the K star give us a spatial probe of the K star's wind. Again, the telling absorptions are in the UV, so most of our knowledge of these stars has come from *IUE* (e.g., Eaton 1996) with incremental improvements from *HST* (e.g., Baade et al. 1996). More recently Harper et al. (2005) have used radio observations of ζ Aur to verify the atmospheric structure they derive from UV lines.

The purpose of this paper is to develop a detailed physical model for the chromosphere/wind of 31 Cyg, to test it, and then use it to interpret observations of emission lines of single stars. There is a commonly held belief, even prejudice, that the chromospheres/winds of single stars are different from those of binary components in that the winds of single stars accelerate much more rapidly than the winds of binaries and reach lower terminal velocities. This paper assesses whether observations of single stars might be consistent with the slower acceleration of binary components. I shall begin with a review of the picture developed for single stars through traditional analyses (Section 2), then discuss the model for cool supergiants developed from observations of the ζ Aur binary 31 Cyg (Section 3), testing it through comparisons with emission lines and radio continuum emission. I then use this model to interpret the measurements for single stars (Section 4) and give some speculations about wind acceleration (Section 5). My approach follows the radically different viewpoint that pressures supporting and accelerating the outer atmosphere are a *microscopic* phenomenon, operating on scales smaller than we resolve with our observations, and are not simply the manifestation of *global* waves.

2. THE GENERAL PICTURE FOR SINGLE STARS

Our observational understanding of single stars consists of several types of data: (1) relative and absolute fluxes of a wide variety of UV and optical chromospheric emission lines, (2) profiles of optically-thin emission lines, reflecting the kinematics of gas forming them, (3) velocity structure of optically thick emission lines, reflecting bulk flows in the chromospheres/winds, (4) line strengths of density-sensitive multiplets, namely C II] UV0.01 λ2325, and (5) strengths of fluorescent lines, reflecting mean intensities in some of the deeper parts of the chromosphere. Many of these results come from *HST* spectra discussed in observational papers by

K. G. Carpenter and his collaborators (Carpenter et al. 1991, 1995, 1997, 1999; Robinson et al. 1998); the more imaginative interpretations of them seem to have come mostly from P. G. Judge (e.g., Judge 1994).

The important results of these papers are (1) measurements of electron density in some part of the emitting region of the chromosphere, (2) turbulent velocities from optically-thin emission lines, (3) possible evidence for multiple components in the profiles of C II], but not other optically-thin lines, as well as in the strengths of fluorescent molecular lines, (4) some indication of the temperatures in the chromospheres/winds from excitation of Fe II and relative strengths of various emission lines, (5) detection of slight amounts of more highly ionized, possibly hotter, gas (e.g., C IV emission), and (6) evidence for atmospheric expansion and a crude measurement of the density–velocity profile from self-reversed Fe II lines and Mg II *h* and *k*.

Chromospheric velocity structure. Many of the weaker intrinsic lines of common elements are weak enough in chromospheric spectra to be optically thin. They should be formed in essentially nebular conditions, with every excitation giving a potentially observable photon, so that their line profiles would reflect the kinematics and ionization structure of the emitting gas. The superior resolution and signal-to-noise ratio of the *HST* have made it possible to measure these profiles reliably. The turbulence measured from such an optically-thin line can be conveniently characterized by a velocity, $v_0 = \mathrm{FWHM}/1.67$, the parameter in the Gaussian part of the velocity distribution [$\exp^{-(v/v_0)^2}$], which Judge (1986a, 1986b) called *b*. Carpenter et al. (1991, 1995, 1997, 1999) fit Gaussians to such lines in a variety of cool stars. We may estimate the turbulence by averaging their results for roughly nine lines between 1900 and 2850 Å, with the C II] multiplet excluded, which give FWHM = 18.2 km s^{-1} (α Tau), 29.9 (λ Vel), 27.2 (α Ori), and 23.6 (γ Cru). I have corrected these values for the 13–15 km s^{-1} resolution of the *GHRS* spectrograph which Carpenter et al. (1991, 1995, 1997, 1999) mention occasionally in passing, except in the cases they explicitly stated that they had corrected their published values. These FWHM's correspond to turbulent velocities in the range v_0 = 10.9–17.9 km s^{-1} for the emitting gas. This is well supersonic for the temperatures expected in these chromospheres ($\lesssim$10,000 K).

The most perplexing result of such kinematic analyses is the existence of broad wings and a ~4 km s^{-1} redshift of the C II] lines in most of these stars. These may well not be formed under similar conditions as most other weak lines, and, in fact, those other lines (such as fluorescent Fe I and weak lines of Fe II and Al II]) do not show these phenomena. This discrepancy implies some sort of anisotropic turbulence seen only in C II] or, perhaps, multiple components in the chromosphere, again not seen in the weak non-C II] lines. Single Gaussians fit to the C II] profiles in the various stars give values of FWHM = 24 km s^{-1} (α Tau), 28 (γ Dra), 36 (λ Vel), 35 (α Ori), and 30 (γ Cru), not corrected for the point spread function (PSF) of the spectrograph. For γ Cru a two-component fit gives FWHM = 27/42 for core/wings; for α Ori, FWHM = 19/48. For λ Vel, the star most like 31 Cyg, we have a characteristic velocity of 21.6 km s^{-1}, presumably uncorrected for the resolution of the spectrograph, or 19.9 km s^{-1} corrected; again, supersonic for the expected chromospheric temperatures. Of particular significance would be any differences of width in these optically-thin lines; if the C II] lines were formed primarily in a different region from the others, they would not necessarily have the same broadening. Indeed, the C II] lines are marginally broader than the other lines in α Tau (ΔFWHM = 1.6 km s^{-1}), λ Vel (3.4 km s^{-1}), and γ Cru (2.7 km s^{-1}). These differences must at least partially reflect the non-Gaussian profiles of C II].

Electron densities. These come primarily from the density-sensitive line ratios of the C II] (Stencel et al. 1981). Electron densities derived from the C II] line ratios in *HST* and *IUE* spectra of typical stars are near 10^9cm^{-3}. It is important to remember that these values apply only to the parts of the chromosphere/wind where the photons are formed. Because C is theoretically expected to be mostly neutral in the deeper reaches of the chromosphere, one might expect that the measured electron densities would apply only to the *warmer* parts of the chromosphere/wind. The C II] lines also give limits on the optical depths of chromospheric gas.

Judge (1994) analyzed the variations of very good observations of α Tau with Doppler shift to derive electron density as a function of velocity. Again, his results were perplexing. They gave higher electron densities, by a factor of 4, for positive velocities (away from us; ostensibly toward the star) than for negative velocities. Furthermore, the emission in α Tau was shifted to the red by 4 km s^{-1}, which Judge interprets as a downflow in the denser regions of the chromosphere. A redshift of 2–4 km s^{-1} seems to be ubiquitous in the cool giants and supergiants (Judge & Carpenter 1998). Upon reflection, that the measured electron density is so similar in all these stars in spite of variations in mass-loss rate of several orders of magnitude (see Harper 1996) is probably just as strange as the line shapes.

Line Strengths. Relative strengths of optically-thin lines give a measure of the mass, temperature, and electron density of emitting gas averaged over the whole chromosphere. They may be interpreted with appropriate empirical or semi-empirical models as Judge (1986a, 1986b) did for several bright stars. This sort of analysis provides global constraints on the integral

$$f_{\mathrm{line}} \sim \int n_{\mathrm{i}} n_{\mathrm{e}} \exp(-\chi_{\mathrm{exc}}/kT_{\mathrm{e}}) dV. \quad (1)$$

Fluxes for characteristic lines come from *IUE* spectra and seem to be roughly consistent from star to star among the cool giants. Such collisionally excited lines as Si II] UV0.01, Al II] UV1, and Mg II *h* and *k* have consistent ratios for cool giants (Judge & Jordan 1991). C II] UV0.01 is not necessarily proportional to the other collisionally excited lines (Judge et al. 1992); however, it is roughly equal in strength to Al II] for most of these stars. For the values given by Judge & Jordan (1991), we can summarize these line strengths as in Table 1. For the windy (noncoronal) giants, the flux in C II] λ 2325.4 seems to be roughly equal to flux in Al II] λ2669. We have also listed strengths for three ζ Aur binaries as best as we can judge them. The Al II] fluxes for these binaries (Eaton 1992) are relatively well determined. The C II] fluxes, however, are very poorly measured and in a noisy part of the *IUE* spectrum. There are no spectra for 31 Cyg exposed long enough to detect this line, and it is hard to differentiate it from the noise in the spectra for ζ Aur and 32 Cyg in which Schröder et al. (1988) claimed to detect it, although Harper et al. (2005) probably detected the strongest component with *HST* in a spectrum dominated by wind-scattered lines. I have given what I consider the best measurements possible for these spectra, but in the following analysis, I shall assume $f(\lambda 2325.4) \approx f(\lambda 2669)$ in all the windy giants. The fluorescent Fe I UV44 lines can be detected in all three classical ζ Aur systems (e.g., Bauer & Stencel 1989), but these two lines, especially λ2844, are highly blended with other features.

Table 1
Line Strengths in Cool Giants and Models

Star	Spectral Type	V $(B-V)$	f(Lyα) $f_{\rm line}/f_V$	f(2325) $f_{\rm line}/f_V$	f(2669) $f_{\rm line}/f_V$	EW(Hα) $f_{\rm line}/f_V$	$\log(n_{\rm e})$
α Boo	K1 III	−0.04	$\geqslant 1.4 \times 10^{3}$	35.7	83.1	1.12	9.7
		1.23	$\geqslant 3.7 \times 10^{-2}$	9.4×10^{-4}	2.2×10^{-3}		
α Tau	K4 III	0.85	$\geqslant 340$	31.3	30.7	1.12	9.0
		1.44	$\geqslant 2{,}0 \times 10^{-2}$	1.9×10^{-3}	1.88×10^{-3}		
β Gru	M5 III	2.13	>50	31.7	28.8	...	8.5
		1.57	$>9{,}7 \times 10^{-3}$	6.2×10^{-3}	5.6×10^{-3}		
λ Vel	K5 Ib-II	2.21	...	...	12	1.52	8.9
					2.5×10^{-3}		
31 Cyg	K4 I	3.79	...	<5	2.3	1.50	...
		1.28		$<5 \times 10^{-3}$	2.1×10^{-3}		
32 Cyg	K4 I	3.98	...	$\leqslant 5 \pm 100\%$	3.4	1.75	...
		1.52		$\leqslant 5.3 \times 10^{-3}$	3.6×10^{-3}		
ζ Aur	K4 Ib	3.79	...	$\leqslant 4 \pm 100\%$	2.2	1.57	...
		1.22		$\leqslant 3.7 \times 10^{-3}$	2.0×10^{-3}		
Model 1 (3% ioniz)			...	56	28	...	9.8
Model 2 (var <10%)			...	9.1	3.6	...	8.5
Model 3 (var < 3%)			...	6.7	3.0	...	8.6

Notes. Line fluxes at the Earth are in 10^{-13} erg cm^{-2} s^{-1}. f(line)/f_V is in Å and assumes $f_V = 3.65 \times 10^{-9}$ erg cm^{-2}s^{-1}Å^{-1} at $V = 0.0$. Values of $\log(n_{\rm e})$ in Column 8 come from C II] multiplet ratios as noted in the text.

Judge (1986a, 1986b; Judge & Jordan 1991) has made simple empirical models for three cool giants, finding that the emission is probably excited in a gas near 7000 K and an electron density of 10^9 (an assumed *global* value of $n_{\rm e}$ from C II] UV0.01). Carpenter et al. (1999) estimated that the Fe II lines observed in the wind of λ Vel are scattered by gas at ∼6000 K from the relative strengths of various multiplets. Other estimates of the electron temperatures of single stars come from adjusting semi-empirical models (e.g., Kelch et al. 1978) to give observed line profiles for characteristic emission lines and Hα absorption.

Fluorescent lines. The classical fluorescent lines of K giants are Fe I UV44 excited by the Mg II *k* line. These lines are optically thick and must be formed in the deeper, denser parts of the chromosphere for any neutral iron to scatter them (Harper 1990). Other fluorescent lines are scattered by molecular species (McMurray et al. 1999; McMurray & Jordan 2000). These molecular species must be present in some part of the chromosphere, but the eclipses of ζ Aur binaries generally do not detect them, probably because there is plenty of cold dense gas in the inner parts of the chromosphere to hide their absorptions in the competing atomic features. McMurray et al. have argued that the strengths of fluorescent H_2 and CO lines, which they could not reproduce with their nondimensional semi-empirical model of α Tau, require a multicomponent atmosphere, possibly with shocks deep in the atmosphere to generate enough Lyα flux there to excite these molecules radiatively.

More highly ionized species. Long exposures in the UV have detected lines of highly ionized species even in the windy giants. These include intersystem lines of Si III and C III (e.g., Carpenter et al. 1999) and the resonance doublet of C IV (e.g., Robinson et al. 1998). In the Sun, such highly ionized species emit lines in the transition region at ∼50,000 K. In the windy giants, this interpretation is problematic because there is no evidence for the coronae that create the transition regions in the dwarfs.

Expansion–velocity structure of the wind. This is very difficult to get from observations of single stars. There is ample evidence of winds in the P-Cyg profiles of Mg II and from the asymmetric, variable profiles of Hα in cool supergiants (Zarro & Rodgers 1983; Mallik 1993). Harper (1996) summarized analyses of wind profiles derived from single stars; Harper et al. (2005) have discussed this in somewhat more detail. Much of the evidence comes from P-Cyg profiles in the UV. Fe II lines of increasing intrinsic strength show increasingly negative velocities of their self-reversals, attributable to wind acceleration, in a number of cool supergiants, notably λ Vel (Carpenter et al. 1999), γ Cru (Carpenter et al. (1995), α Ori (Carpenter & Robinson 1997), and both α Tau and γ Dra (Robinson et al. (1998). Of these, λ Vel had the most extensive coverage of the accelerating wind, with centers of the shell lines shifted to ~ -32 km s^{-1} with respect to the star, and Carpenter and Robinson have interpreted the data for these stars to infer mass-loss rates, terminal velocities, level of turbulence, and density structure. Such analyses give winds accelerating much faster than those of the ζ Aur binaries or, for that matter, of *single* stars as deduced from radio observations (Harper et al. 2001, 2005; Carpenter et al. 1999). In fact, the analysis of thermal radio emission has become a fruitful technique for deducing the wind structure of single windy giants (e.g., Drake & Linsky 1986; Harper et al. 2001).

3. THE MODEL FOR 31 CYG

Although optical spectra provided many insights into the nature of the extended atmospheres of the cool supergiant components of ζ Aur systems, the field was essentially dormant from the mid-1950s until *IUE* revitalized it with panchromatic UV spectra. I have discussed the results of such studies in a review at the Cool Stars 9 meeting (Eaton 1996). I shall summarize them here as follows. First, the new UV observations recorded absorptions from most of the important species expected to exist in the chromospheres and winds of cool giant stars. In contrast, optical spectra give very few of these species. Furthermore, these UV absorptions are often intrinsically strong lines that can be detected at great heights above the stellar surface, giving

us the ability to probe winds to much greater height. For the first time we could use the wings of Lyα to measure hydrogen column densities directly for many lines of sight through the wind/chromosphere. The many lines of Fe II, likewise, gave measurements of excitation temperature ($T_{\rm exc} \sim$ 5000–12,500 K) and kinematics of the wind throughout much of the wind and upper chromosphere.

Some of the results from *IUE* are conventional while others are surprising. Strengths and shapes of lines from different ionization stages of metals, most importantly iron, confirm the expectation that the metals are mostly *singly-ionized* throughout the chromospheres and winds of these stars. Likewise, the detection of the wings of Lyα at height in chromospheres and rough agreement of the mass column densities derived with those from Fe II means that *H is primarily neutral* throughout those parts of the wind we can sample. This contradicts the predictions of semi-empirical models in which H becomes completely ionized over the first several scale heights of the chromosphere, giving roughly a constant electron density in the line-emitting regions in spite of a marked decrease of total density (Judge 1990, p. 290; Section 3.2). This observation that H remains neutral thus places limits on permitted kinetic temperatures and local electron densities in the gas. Furthermore, wind models for 31 Cyg give us some direct insight into the turbulence in chromospheres. Single-component models of the gas with no expansion effects, i.e., the sort of analyses used by Wilson & Abt (1954), find Doppler widths of the order of 20 km s^{-1}, decidedly supersonic for gas with kinetic temperatures below 10,000 K. *IUE* observations show that at least some of this spread is caused by the differential expansion of the gas along the line of sight and need not be attributed to local turbulence. In fact, the *IUE* observations for 31 Cyg require a turbulence $\lesssim$15 km s^{-1}.

Even in the classical optical analyses, the ionization of metals was lower than expected for a uniformly distributed gas and thereby implied clumping for the gas to achieve enough electron density to maintain an observable population of trace neutral species, such as Fe I. UV observations confirm this result. Ionization throughout the wind is lower than expected from simplistic calculations of ionization equilibrium and implies clumping in the range 10–30 $\times$ to achieve the inferred electron densities ($n_{\rm e} \sim$ 0.2–1.5 $\times$ 10^9 cm^{-3} in the inner 150 $R_\odot$ of the chromosphere). This is a complication well beyond most semi-empirical models of chromospheres.

We can use an idealized description of the measured physical properties of the gas in the chromosphere and wind of 31 Cyg to test ideas about the structure of chromospheres and, ultimately, about wind mechanisms. These measurements are based on the most extensive set of observations ever obtained for a ζ Aur binary (Eaton & Bell 1994). I have chosen to concentrate on 31 Cyg over the years because it has a much longer period than the other two classical ζ Aur binaries (ζ Aur and 32 Cyg). This gives it a greater separation and less interaction between the wind and B star, a big advantage in many analyses. The wind-scattered emission lines seen in total eclipse, for instance, are weaker than in the other two stars (Eaton 1992). I am adopting the following properties for the 31 Cyg system: D = 473 pc, $R_{\rm K}$ = 197 $R_\odot$, $M_{\rm K}$ = 11.7 $M_\odot$, $M_{\rm B}$ = 7.1 $M_\odot$, v_∞ = 90 km s^{-1}, $\dot{M}$ = 3.0 $\times$ 10^{-8} $M_\odot$ yr^{-1} (Eaton 1993c; Eaton & Bell 1994). We should note that, in observing the more complicated ζ Aur, Baade et al. (1996) probably had a better case than 31 Cyg for applying their wind-scattering analysis. Furthermore, inasmuch as the models for 31 Cyg and ζ Aur give essentially the same results in terms of velocity structure/extension of the wind and wind temperatures, we can be confident that the results for either of them should be readily applicable to other stars.

Table 2 gives the details of the empirical chromospheric/wind structure I am using to test wind models. Quantities listed are (1) radius (distance from the center of the star in $R_\odot$), (2) expansion velocity, (3) excitation temperature, (4) a temperature to drive the wind thermally, (5) a clumping factor, CF, giving the inverse of the fraction of space actually filled with matter, (6) log($n_{\rm H}$), the total hydrogen density, (7) log($n_{\rm e}$), the local electron density from an assumed constant ionization of H (3%) and amount of clumping, (8) log($n_{\rm e}$) for the variable ionization developed in Section 3.2 and with the assumed clumping, but limited to 10% in the outer chromosphere, and (9) $v_{\rm equ}$, a velocity derived from equipartition between mass motion and internal thermal energy of the gas (see Section 5.2).

Now we come to the crux of this paper in that, for the first time, it relates the mechanism driving the wind to the wind's clumping and physical structure in a way giving testable predictions. Although the electron densities measured from photoionization balance imply significant clumping of the gas, they are rather crude and may be systematically wrong. An independent way to estimate this degree of clumping is to look at the difference between the pressures[1] required to drive the observed wind and the gas pressures that would be available in the wind if it were not clumped. This approach works because the gas pressures ($\sim \rho T_{\rm gas}/\mu$) would be in equilibrium with whatever pressure drives the wind. We do this by determining a temperature structure to drive the observed wind *thermally*, as though these stars had a coronal, i.e., generalized Parker-type, wind (see Lamers & Cassinelli 1999, Chapters 4 and 5), then comparing those temperatures to the observed temperatures, point by point, assuming that the excitation temperatures we have measured approximate the electron temperature. This last assumption seems reasonable because the excitation temperatures are similar to temperatures derived for semi-empirical chromospheric models of single stars, at least in the inner parts of the wind, but we will test it in later sections. To reiterate, if the gas is clumped, thereby bifurcating into dense clumps and an unspecified interclump medium, there must be a pressure in the interclump medium maintaining the clumping. We will assume that this is the pressure driving the wind and that it somehow breaks the wind up into microscopic clumps and maintains them. This is fundamentally different from the approach of traditional wave models in which the gas is uniform and the waves act on it continuously.

The temperature structure to produce the pressure gradient required to drive the wind of 31 Cyg thermally, which we have derived from a thermal-wind model, is given roughly by the equations

$$T_{\rm therm} = 20{,}000\,{\rm K} + 75{,}000\,{\rm K}(r - R_*)/R_* \quad \text{for } (r - R_*) \times < 150\,R_\odot, \tag{2a}$$

and

$$T_{\rm therm} = 95{,}000\,{\rm K} - 75{,}000\,{\rm K}(r - 3R_*)/(15R_*) \quad \text{for } (r - R_*) \times > 2R_*, \tag{2b}$$

[1] Strictly speaking, the wind is driven through the pressure *gradient*, which appears in the hydrodynamical momentum equation ($F = ma$), but a given pressure distribution, the higher level abstraction I am specifying, implies a pressure gradient, even in the simplistic case of an isothermal wind.

Table 2
Details of the Model for 31 Cyg

R	$v_{\rm exp}$	$T_{\rm exc}$	$T_{\rm therm}$	CF	$\log(n_{\rm H})$	$\log(n_{\rm e})$ (3%)	$\log(n_{\rm e})$ (var)[a]	$v_{\rm equ}$
(1)	(2)	(3)	(4)	(5)	(6)	(7)	(8)	(9)
7000.0	83.8	12500.	20000.	1.60	4.53	3.21	3.73	11.3
6200.5	83.0	12500.	20000.	1.60	4.64	3.32	3.84	11.3
5466.3	82.1	12500.	20000.	1.60	4.75	3.43	3.95	11.3
4794.5	81.0	12500.	20000.	1.60	4.87	3.55	4.07	11.3
3897.8	79.1	12500.	20000.	1.60	5.06	3.74	4.26	11.3
3369.9	77.4	12500.	24468.	1.96	5.20	3.96	4.49	12.5
3126.0	76.5	12500.	30660.	2.45	5.27	4.13	4.66	14.0
2894.9	75.5	12500.	36526.	2.92	5.34	4.28	4.80	15.2
2676.2	74.3	12500.	42075.	3.37	5.41	4.42	4.94	16.3
2469.7	73.1	12500.	47316.	3.79	5.49	4.55	5.07	17.3
2275.0	71.8	12500.	52258.	4.18	5.57	4.67	5.19	18.2
2091.8	70.3	12500.	56909.	4.55	5.65	4.79	5.31	19.0
1919.7	68.7	12500.	61278.	4.90	5.74	4.90	5.43	19.7
1758.3	66.9	12500.	65374.	5.23	5.82	5.02	5.54	20.4
1607.3	64.9	12500.	69206.	5.54	5.92	5.14	5.66	21.0
1466.4	62.8	12500.	72783.	5.82	6.01	5.25	5.77	21.5
1335.2	60.4	12500.	76113.	6.09	6.11	5.37	5.89	22.0
1213.3	57.8	12500.	79205.	6.34	6.21	5.49	6.01	22.4
1100.5	55.0	12306.	82068.	6.67	6.32	5.62	6.14	22.8
996.4	51.9	11902.	84712.	7.12	6.43	5.76	6.28	23.2
900.6	48.5	11508.	87143.	7.57	6.54	5.90	6.42	23.5
812.7	45.0	11103.	89373.	8.05	6.67	6.05	6.57	23.8
732.5	41.1	10709.	91408.	8.54	6.80	6.20	6.73	24.1
659.6	37.1	10308.	93259.	9.05	6.93	6.37	6.89	24.3
593.6	32.8	9910.	94934.	9.58	7.08	6.53	7.06	24.6
534.2	28.5	9515.	95000.	9.98	7.23	6.71	7.23	24.6
481.1	24.1	9133.	95000.	10.40	7.39	6.89	7.41	24.6
433.8	19.8	8755.	95000.	10.85	7.57	7.08	7.60	24.6
392.2	15.7	8388.	95000.	11.33	7.76	7.29	7.81	24.6
355.7	12.0	7193.	95000.	13.21	7.96	7.56	7.78	24.6
324.04	8.66	6830.	83520.	12.23	8.18	7.75	7.76	23.0
296.92	5.92	6492.	69960.	10.78	8.42	7.93	7.74	21.1
273.96	3.77	6178.	58482.	9.47	8.69	8.14	7.77	19.3
254.82	2.36	5883.	48912.	8.31	8.95	8.35	7.81	17.6
239.15	1.44	5625.	41077.	7.30	9.23	8.57	7.87	16.2
226.61	0.81	5410.	34803.	6.43	9.52	8.80	7.98	14.9
216.83	0.42	5244.	29917.	5.70	9.84	9.08	8.16	13.8
209.49	0.20	5105.	26245.	5.14	10.20	9.39	8.39	12.9
204.23	0.11	4998.	23614.	4.72	10.48	9.63	8.57	12.2
200.70	0.06	4930.	21850.	4.43	10.75	9.87	8.77	11.8
198.56	0.04	4905.	20781.	4.24	10.94	10.04	8.92	11.5
197.46	0.04	4905.	20231.	4.12	10.98	10.07	8.95	11.3
197.06	0.04	4905.	20029.	4.08	10.98	10.07	8.95	11.3
197.00	0.04	4905.	20000.	4.08	10.98	10.07	8.95	11.3

Note. [a] Ionization as in Figure 5 but limted to 10% in the outer chromosphere.

where $T_{\rm therm}$ is thermal (electron) temperature for a uniformly distributed gas, r is the radius, and $R_* = 197\,R_\odot$ is the photospheric radius of the star. I do not claim that this structure is a rigorous determination of the thermal-pressure profile, but that it is adequate for giving a good idea of the pressures required throughout the wind. Figure 1 shows the velocity structure calculated for this adopted temperature structure of Equation (2), and Figure 2 shows the amount of clumping implied.

A way to test this sort of model is to calculate the emission expected from it. I have done this in two ways: first, with a spherically symmetrical model that calculates the line strengths, line profiles, and chromospheric mass column densities specifically for 31 Cyg. The second way uses a traditional plane-parallel model for ζ Aur I developed in 1992–1995 with PANDORA (Vernazza et al. 1973; Avrett & Loeser 1992) to explore the ionization structure and effect of clumping in these stars.

3.1. Tests of a Spherically Symmetrical Model for 31 Cyg

The spherical model for 31 Cyg has the distribution of gas given in Table 2. The velocity structure and distribution of mass density (given as $n_{\rm H} = \rho/1.4m_{\rm H}$) come from fitting spectra of shell lines in atmospheric-eclipse spectra; they should be fairly reliable. Excitation temperature comes from fitting the excitation of Fe II in these atmospheric-eclipse spectra; they should be reliably measured but subject to uncertainty about their meaning. Electron densities depend on the level of ionization of H and degree of clumping. We can make educated speculations about these properties as follows. Since H seems to be neutral observationally, we might expect the ionization

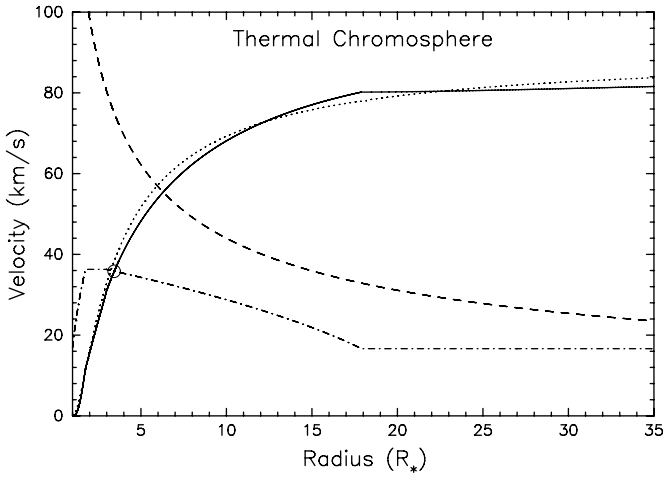

Figure 1. Coronal wind model to fit the derived velocity structure of 31 Cyg. The dotted line is the velocity profile derived for 31 Cyg by Eaton & Bell (1994), while the solid curve is the velocity profile calculated with the temperature profile of Equation (2). Other curves are the local escape velocity (dashed) and sound speed for the velocities in Equation (2) (dot-dashed). The circle shows the sonic point in this model.

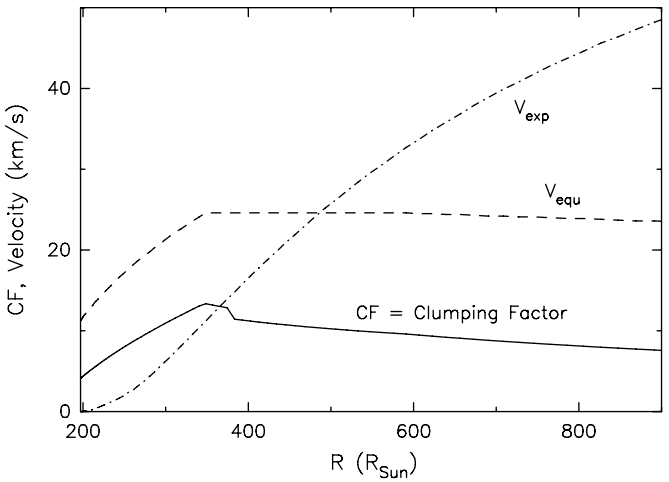

Figure 2. Inferred clumping for the 31 Cyg model. The solid curve is the calculated clumping factor, CF, and the dashed line is the equipartition velocity defined by Equation (7). The atmospheric expansion velocity, $v_{\rm exp}$ is shown for comparison.

to be $\lesssim$10%. We will assume it stays constant with height, following the thoughts of Judge (1990, Section IIIb), and of the order of 1–5%, and adopt a value of 3% for the sake of a first-order model. In that case, the gas must be clumped even to approach the canonical C II] electron density almost anywhere in the chromosphere.

3.1.1. Line Emission

For optically-thin lines, we can calculate the emission with the standard physics given by Osterbrock (1974), for example, with assumptions about ionization and chemical abundances. In this approximation, emissivity [erg cm^{-3} s^{-1}] is just

$$\epsilon_\nu = 8.63 \times 10^{-6}\, \Omega_{1,2} n_{\rm i} n_{\rm e} \exp(-\chi/kT) T^{-0.5} \omega_{\rm l}^{-1} \chi \qquad (3)$$

where $n_{\rm i}$ is the density of emitting ions, Ω is the collision strength, χ is the excitation energy of the upper level, and $\omega_{\rm l}$ is the statistical weight of the lower level. In this approximation, emission is proportional to collision strength, and we have incorporated collision strengths for C II] λ2325 (Ω = 0.830 and 1.66, for transitions out of the two ground-state levels, with half the emission going into the dominant 2325.4 Å line) from Blum & Pradhan (1992) and for Al II] λ2669 (Ω = 3.3) from Tayal et al. (1984). The abundances of C and Al were $A_{\rm C}/A_{\rm H} = 2.0 \times 10^{-4}$ and $A_{\rm Al}/A_{\rm H} = 3.0 \times 10^{-6}$ (Eaton & Bell 1994, Section 2.1). To determine the total emission in an optically thin line as a function of radius on the sky, we sum the emissivity along a ray through the atmosphere, with integration limits determined by whether or not it intersects the star. To get a profile for the line, we define a velocity scale and map the emissivity profile of the gas at each point in the atmosphere onto it, with allowance for the atmospheric expansion, $v_{\rm exp}$, an arbitrary (systematic) velocity along the line from the center of the star, $v_{\rm syst}$, and a spectrum of Gaussian turbulence, v_0.

The first thing we note from these models is the effect of the extended spherical atmosphere on the emission strength and line profiles. Optically thin lines formed in such a structure will be highly *limb brightened*, and will combine contributions from the face of the star and from a halo beyond its limb in similar proportions. Figure 3(a) illustrates this effect for our 31 Cyg model for an emitter assumed to exist in the same ionization stage throughout the wind ($n_{\rm e}$ as in Column 7 of Table 2). The emission peaks somewhat more to the limb than mass because electron density drops rapidly with height in these atmospheres, even with the assumed clumping. An emitter that is depleted in the inner chromosphere, as C II] may be, would peak even further beyond the limb. This is shown in the figure as a dashed line calculated for emission only at temperatures in the model above 5200 K. Even so, most of the emission would come from within the first $\lesssim$ 0.15 R_* of the chromosphere/wind. Strong resonance lines, however, should be *limb darkened*. Scattering in an extended atmosphere would give a highly forward-peaked source function (e.g., Cassinelli & Hummer 1971), the reason for the core–halo profile of the disks of W-R stars, and, for resonance lines in chromospheres, the large optical depths mean the escape probability for photons migrating through the damping wings would be much smaller for the radial direction than for other lines of sight.

Simple calculations, like those in Figure 3(a), cannot represent the conditions in actual chromospheres because they give *fluxes* much higher than observed. Table 1 gives fluxes calculated for three cases: (1) uniform 3% ionization of H, (2) variable ionization of H, limited to 10%, and (3) variable ionization of H, limited to 3%. The model with uniform H ionization arbitrarily set at 3% gives an Al II] flux too high by a factor of 10 and a C II] flux at least as bad. By contrast, the model with variable ionization (Table 2, Column 8), gives Al II] flux high by ~50% and C II] high by slightly more, but the high electron density in the outer winds of these models, combined with single ionization of metals, gives much larger line broadening from differential expansion of the atmosphere. These models also have problems with electron density. If we average $n_{\rm e}$ over emission of C II], the values are either too high, as for the calculation for the unrealistic uniform 3% ionization of H, or somewhat low, as for the realistic ionization of H limited to 3% or even 10%. Figure 3(b) shows the intensity profiles for the model with variable ionization. The effect of the 10% ionization in the wind is obvious, with much of the emission in the wind coming from the hot ionized outer parts. These parts, however, have electron densities much too low (7.7 in the log) to give the C II] line ratios,

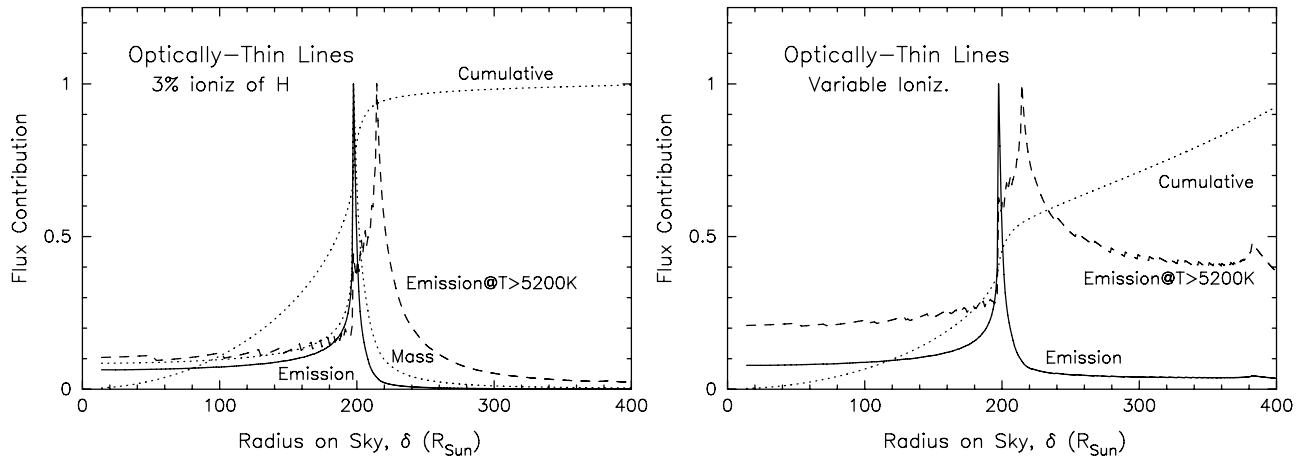

Figure 3. Calculated intensity of emission over the stellar disk for optically-thin emission lines. Left: this figure assumes the emitter is in the same ionization stage throughout the chromosphere (n_e in Column 7 of Table 2). Right: this figure is for the more realistic level of ionization (n_e in Column 8 of Table 2).

at least those seen in single stars, and they produce C II] profiles much broader than observed. They are clearly inappropriate for single stars unless C becomes *doubly ionized* in the outer wind or unless the temperature in the outer wind is well below the measured excitation temperatures.

3.1.2. Radio Continuum Emission

A further test of these spherical models comes from the radio continuum observations of Drake & Linsky (1986) and Drake et al. (1987), who detected a number of bright cool supergiants at the 0.1 mJy level (or 10^{-27} erg cm^{-2}s^{-1}Hz^{-1}). Their measurement for 31 Cyg (0.36 ± 0.07 mJy) gives a check on the consistency of the electron densities and temperatures we are assuming. The basic idea (see Harper et al. 2005) is to integrate the radio source function, $S_\nu = B_\nu$, along rays through the wind and then sum the resulting intensities over the stellar disk to get a kind of luminosity [erg s^{-1} ster^{-1}Hz^{-1}]. This quantity would then be converted to flux at the Earth by multiplying it by the solid angle of 1 cm^2 at the star's distance, D. The dominant free–free opacity from electron–proton interactions, corrected for stimulated emission, is just

$$\kappa_\nu = 0.212 n_p n_e T_e^{-1.35} \nu^{-2.10} \quad (4)$$

(Harper et al. 2005, Equation (3)), while the generally smaller contribution from neutral-hydrogen–electron interactions (H^-) is roughly

$$\kappa_\nu = 6.2 \times 10^{-35} n_H n_e (\lambda/1\,\mathrm{cm})^2 T_e \quad (5)$$

(Allen 1973, Section 42 evaluated at 8000 K). For the values of T_e, CF, n_e in Table 2 (Column 8 for n_e), we calculate a flux at the Earth of 0.04 mJy at 6.2 cm, only about 10% of the amount measured by Drake et al. Figure 4 shows the calculated intensity profile, a slightly limb-brightened disk with a radius of $\sim$3.8 R_*. This failure to reproduce the flux seems to be a common problem in reconciling the radio emission of cool giants with their UV spectra. Carpenter et al. (1999), for instance, were unable to reproduce the 3.5 cm flux of λ Vel with the rapid wind acceleration they found from UV lines. Harper et al. (2005), likewise, were unable to reproduce the radio spectrum of ζ Aur with their model and found it hard even to get the flux level.

To get emission as great as is observed for 31 Cyg, the outer wind must be essentially wholly ionized, as the large mass-loss rate of Drake et al. (1987) implies. If we let the outer

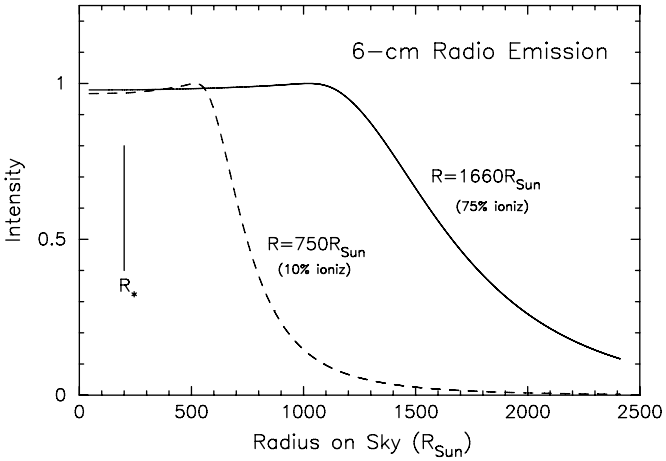

Figure 4. Calculated intensity of 6.17 cm radio emission over the stellar disk for two models: dashed curve for the model with variable ionization limited to 10% (n_e in Column 8 of Table 2) and solid curve for the same model with 75% ionization of H in the outer atmosphere. This latter distribution would project a disk of 38 mas and have a spectral index $\alpha = 1.08$, comparable to the few values measured by Drake & Linsky (1986).

wind become mostly ionized, we can at least approach the flux level observed. For instance, with H in the envelope 75% ionized above 8000 K, we get a flux of 0.22 mJy; for 100% ionization, 0.28 mJy. Is this level of ionization reasonable? It seems consistent with observations of ζ Aur stars, especially 31 Cyg, but the evidence for single stars is ambiguous. Such high ionization should reveal itself through absorptions of *doubly* ionized species in spectra of ζ Aur binaries and possibly through emission lines from these species in both the binaries and single supergiants. The broadening of these lines would be a measurement of the terminal velocity and turbulence of the outer wind. Let us look at the observations of these species in some actual stars. There is a weak emission feature at the position of Si III] λ1892 in the eclipse spectra of 31 Cyg (*IUE* images SWP47335 and SWP47336). In addition, strong emission lines of higher ionization are seen in eclipse in all three classical ζ Aur binaries. Multiplets Al III UV1 and Fe III UV34 in 31 Cyg have P-Cyg profiles (Bauer & Stencel 1989, Figure 3) and are so strong that they must be formed by scattering of light from the B star in the wind. The line widths at the bases of their profiles are roughly 170 km s^{-1}, about what one would expect for a

wind at terminal velocity. Eaton & Bell (1994) found that these absorptions are formed primarily at velocities *toward the B star* and likely result from the ionization of the outer wind by the B star, not by intrinsic radiation of the supergiant. Thus a large fraction of the outer wind is ionized *in the 31 Cyg system*. Since H requires less energy to ionize than the 19 eV to ionize C^+ out of its metastable level, H is likely ionized, as well, in these regions of 31 Cyg.

Single stars may have lower ionization in their outer winds than the binaries with similar mass-loss rates, although there is evidence in P-Cyg profiles of wind lines that some of the metals are doubly ionized in many of them (see Section 4.2). Carpenter et al. (1999) detected lines of C III] and Si III] in λ Vel with about the right broadening and strength to be formed in an ionized wind. However, they interpreted these lines as an indication of gas at ∼50,000 K, as though high ionization necessarily means high temperature. The problem with wind formation is that the computed line profiles are wrong. The calculated profiles are essentially square, having a central dip reflecting the absence of gas at low expansion velocities, while the observed profiles, although somewhat noisy, seem to have a central peak as though formed at least partly in turbulent gas at low expansion velocity. Therefore the *emission* lines of single stars unfortunately tell us nothing about the ionization of their outer winds.

3.2. Calculations with PANDORA

PANDORA is useful for exploring nontraditional models of chromospheres because it lets one specify an arbitrary distribution of turbulence to increase the scale height in hydrostatic equilibrium and to specify an arbitrary distribution of added electron density that can be used to simulate clumping. I have made exploratory calculations for three cases: (1) a chromosphere for ϵ Gem (G8 Ib) based on the model of Basri et al. (1981), (2) a generalized model of a ζ Aur binary ($R_* = 150\ R_\odot$) with temperatures and scale heights based on my analyses of ζ Aur (Eaton 1993a) and 32 Cyg (Eaton 1993b), and (3) models for α Tau to explore excitation of Hα in cool giants (Eaton 1995). In the paper about Hα, I explored the conditions necessary for exciting Hα and C II] in semi-empirical hydrostatic models, finding that a certain amount of clumping of the warmer gas was required to strengthen Hα and to have electron densities high enough to give reasonable C II] line ratios.

These semi-empirical models can give us some insight into how the gas might be ionized at various depths in actual chromospheres. All the models, regardless of assumptions about scale height, clumping, and temperature, predict species such as Al will be singly ionized throughout the whole emitting atmosphere. For H and C, the calculated ionization increases with height. Figure 5 shows this effect for H. In it, I have parameterized height with the electron temperature, since, by assumption, temperature increases monotonically with height above a temperature minimum in all such semi-empirical models. The calculations show that $\log(n_e/n_H)$ increases from a minimum of −4.0 at ∼2600 K, determined by ionization of the metals included in the calculation, to 0.0 (complete ionization of H) at ∼9400 K. For C, complete ionization occurs near 5000 K in these models. The actual models have scale heights somewhat smaller than that of 31 Cyg, so the level of ionization could be higher in 31 Cyg.

3.3. A Further Question about the 31 Cyg Model

One possible error in Eaton & Bell's (1994) analysis of 31 Cyg is the determination of the temperature from excitation

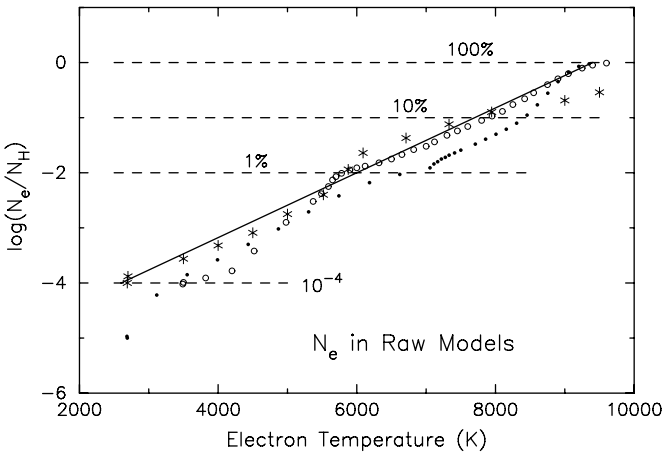

Figure 5. Calculated ionization in three semi-empirical models for cool giant stars. The graph gives the ratio of electron density to total H density as a function of temperature. At low temperature, where ionization of H is low, the electron density is dominated by metals. At high temperature H becomes completely ionized, in these models, if not in actual stars. The region in which most of the chromospheric lines are emitted has an H ionization of a few percent. The solid curve shows the relation I have adopted to relate electron density to excitation temperature in the calculations with variable ionization of H. Discrete symbols represent calculations for three models: dots, α Tau (Eaton 1995: Table 4, Model t8), circles, ϵ Gem, and asterisks, ζ Aur.

of Fe II. We have assumed that the excitation temperatures measured are bona fide electron temperatures of the gas. This might be the case, in that most of these lines arise from excited metastable levels which would probably be in thermal equilibrium with the electrons, at least in the denser parts of the wind (e.g., Judge et al. 1992). Harper et al. (2005) argued this point explicitly, while others deriving temperatures for ζ Aur binaries (such as Eaton & Bell) have implicitly assumed it. However, the excitation temperatures in the outer parts of the winds may well be greater than the thermal temperatures, since these regions are bathed in the radiation of a B star, and since the electron densities expected in these zones are lower than the critical density (∼10^6 per Judge et al. 1992) for radiative processes to become important. In the model for 31 Cyg, these temperatures have very little effect on the emission at any wavelength, since the densities are very low.

Contrariwise, all of these stars have rather high excitation temperatures in their outer chromospheres, regardless of the effective temperature of the B companion. We see this in Figure 6 which gives T_{exc} as a function of tangential mass column density through the chromosphere. We see that the temperature rises to about 8500 K where the Balmer lines become optically thin. This agrees roughly with theoretical calculations for supergiants.

4. IMPLICATIONS FOR *SINGLE* STARS

Here I shall attempt to fit the rich lore of space-dimensionless analyses of line emission and absorption of single stars into the context of our knowledge of the legitimately one- to two-dimensional knowledge of ζ Aur binaries. We might expect the wind structure of the binaries to be essentially the same as that of single stars because the strengths of intrinsic emissions formed in the wind and chromosphere of ζ Aur binaries are similar to those of single stars (Schröder et al. 1988; Eaton 1992; Harper et al. 2005, Figure 6), and the Hα profiles, and their variation, seem to be the same as well (Eaton 1995; Eaton & Henry 1996).

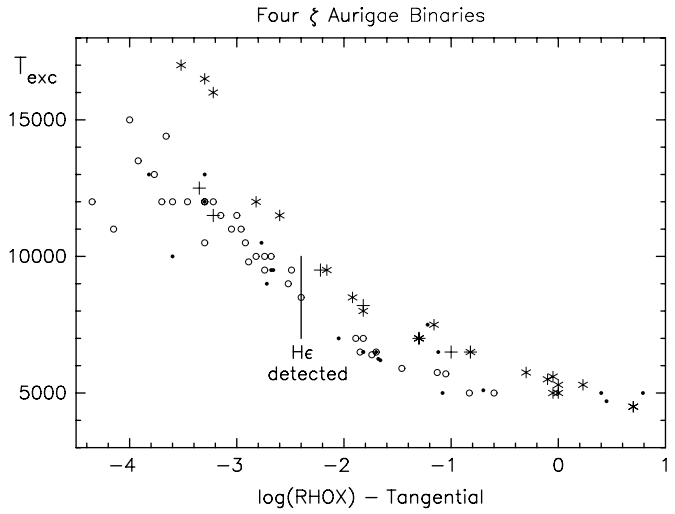

Figure 6. Excitation temperature, $T_{\rm exc}$, vs. tangential mass column density, $\int \rho \, dx$, as measured in four ζ Aur systems. Plusses are for ζ Aur, asterisks for 32 Cyg, circles for 31 Cyg, and dots for 22 Vul.

4.1. The Reality of Semi-Empirical Models

Most detailed analyses of cool stars' chromospheres are based on semi-empirical models in which one posits a temperature rise through the outer atmosphere, calculates a density structure from hydrostatic equilibrium and radiative transfer, and then calculates the emergent spectrum from the physical conditions derived (e.g., Kelch et al. 1978; Basri et al. 1981; McMurray 1999). These models are inspired by the solar chromosphere, in which there is a temperature rise from a minimum, determined by the location where non-radiative heating begins to dominate heating by photospheric radiation, to a point where the chromosphere merges with a transition region of rapidly increasing temperature, heated by downward conduction from a corona. The increase in temperature with height follows naturally from observations of the Sun and from the physical consideration that temperature should rise with decreasing density to keep emissivity from falling precipitately with height per Equation (1). Of course, there might be other ways to organize a chromosphere. For example, the material at different temperatures might be more intimately mixed throughout the chromosphere, as McMurry et al. (1999) contemplate to some degree. Harper et al. (2001), likewise, have speculated about a truly radical reinterpretation of α Ori in which the chromospheric line emission comes entirely from hot inclusions in a generally cool neutral wind, although Harper et al. (2005) did not attempt to apply this radical approach to ζ Aur. Indeed, temperature measurements for ζ Aur binaries, at least to first order, confirm some sort of general temperature rise with height. Figure 6 shows the relation between excitation temperature and tangential mass column density through the atmospheres for four stars. The temperature rise is obvious. While this evidence does not preclude mixing some hot gas with the bulk of the warm gas throughout the chromosphere, it shows that the bulk of the gas behaves sort of like the gas in these classical semi-empirical models.

Another fundamental property of semi-empirical models is the density structure. In the calculated models, it usually comes from hydrostatic equilibrium between gravity and thermal motions of the emitting gas ($T < 10{,}000$ K). This is problematic in that there are obviously other sources of momentum flux in a typical chromosphere, such as the turbulence we see in profiles of emission lines, which will extend the atmosphere, changing its mass and electron density structure. Furthermore, the mere existence of turbulence implies some sort of clumping of the gas, which would necessarily change the local electron densities and ionization structure. Moreover, such effects would change the transfer of radiation and escape of photons from the chromosphere.

A third property of many semi-empirical models is a precipitate temperature rise to coronal temperatures defining the top of the chromosphere. This is not a necessary feature, especially in the windy giants. Nevertheless, McMurry (1999) used such a rise for α Tau to fit the Lyα profile and calculate emission from highly ionized species. However, the observations of ζ Aur binaries do not require such a rise and may not even allow it; the profiles of C III] and Si III] seem to require formation at least partly in the inner chromosphere/wind, and the arguments of McMurry et al. (1999, 2000) suggest there are other places to excite C IV.

4.2. Terminal Velocities of the Winds

One of the basic tenets of our understanding of the windy giants is the idea that their terminal velocities are much lower than the surface escape velocity (e.g., Hartmann & McGregor 1980; Judge 1992; Harper 1996). These terminal velocities are probably not as well known as we think they are, and they may well be *much* higher than generally thought, especially in normal K giants such as α Tau, as Judge (1992) argued in a provocative paper about wind energetics. This is hardly a new idea (see Judge 1992; Ahmad & Stencel 1988; Kuin & Ahmad 1989), but it is certainly worth discussing further in the context of supposed differences between single stars and binary components. For the classical ζ Aur binaries, we base the terminal velocity on measurements of shell lines seen at all phases (e.g., Eaton 1993c). We should be suspicious of low terminal velocities since the metals in the outer parts of the winds might well be doubly ionized, as they are in calculations of Harper et al. (2005, Figure 5) for ζ Aur and Section 3.2 above for single stars. Furthermore, the recombination time for H, given the electron densities in the outer parts of our model ($\sim 10^{3-5}$cm^{-3}), is of the order of 1–100 yr. Semi-empirical models for single stars also become fully ionized, at least in H, in these regions, if that actually means anything. So we really do not know what these winds are doing in a vast volume of space before they recombine and form the shell lines. Occasionally more of the velocity structure may reveal itself through abnormally dense winds, as in AL Vel in 1992 (Eaton 1994, Figure 8) and in λ Vel in 1990 (Mullan et al. 1998). Furthermore, we should realize that the winds must be sweeping up interstellar gas in these shells (see Wareing et al. 2007). This means that the shell velocities are, if anything, likely to be *lower* than the true terminal velocities.

Carpenter et al. (1999) admit that we probably do not see much of the velocity structure in the traditional shell lines in many stars, while they contend that they have seen it all in λ Vel. However, it is not clear from the line profiles of Mg II, O I UV2, and Fe II UV1 that one sees it even in that case. The velocity structure for λ Vel in 1994 seems to be ionization bound, with the maximum wind velocity sampled limited by ionization of Fe^{+} to Fe^{+2}. In an ionization-bound wind, the relatively high density behind the ionization front would allow somewhat weaker lines to become thick at their normal rate, while the strongest lines would quickly saturate at the velocity of the ionization front, little more than the velocity of those somewhat weaker lines, to give the sort of leveling off seen in the highest measured velocities. The edge velocities for all these

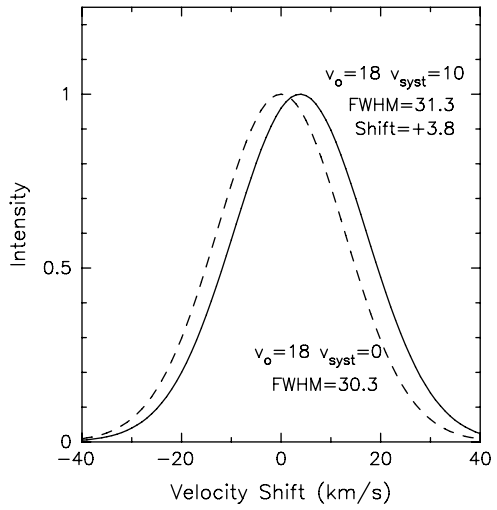

Figure 7. Line profiles for the spherical model for two typical ions. The dashed curve shows the calculated profile for a line like Al II] excited throughout the chromosphere with an isotropic turbulence of 18 km s^{-1} superimposed on the expansion of the chromosphere/wind. This profile is fit to within the resolution of the plot by a Gaussian with FWHM = 30.3 km s^{-1}. The solid curve shows the effect of superimposing a global 10 km s^{-1} downdraft on this profile. It is again fit with a Gaussian (no C II]-like wings) but shifted 3.8 km s^{-1} to the red and broadened slightly to FWHM = 31.3 km s^{-1}.

strong lines in 1994 are around 50 km s^{-1}, much greater than the supposed terminal velocity of 33 km s^{-1}. Furthermore, in 1990 the star showed absorptions to at least 80 km s^{-1} (Mullan et al. 1998), which places its terminal velocity close to what we think 31 Cyg has, if the increase really did come from lower ionization in the outer wind. Also, in comparing α Tau and γ Dra, Robinson et al. (1998) found terminal velocities of 30 and 67 km s^{-1}, respectively, for stars that otherwise seem to have similar atmospheric structure. All this evidence suggests terminal velocities several times as large as they often seem, with the *apparent* terminal velocity dependent on just how much material is being ejected into the flow at a given time.

There is another problem in interpreting these shell lines (see edge velocities of λ Vel) that would lead to errors in the terminal velocity. Carpenter et al. (1991, 1995, 1997, 1999) have interpreted the widths of Gaussians fit to the shell lines as a measure of *turbulence*. This could conceivably be the case for Fe II, but it is clearly inappropriate for at least some lines, for instance, for Mg II in γ Cru (Carpenter et al. 1995; Figure 10), where Mg II seems to have a significantly lower expansion velocity than even moderate Fe II lines. Such corrections for wind turbulence seem wrong, from both observational and theoretical considerations. Observationally, in models for scattering in shells (e.g., Baade et al. 1996), the turbulence drops with height. Theoretically, one would expect the turbulent energy to go into accelerating or heating the wind and be essentially damped out by the time the wind reaches its terminal velocity.

4.3. Turbulence of the Chromospheric Gas

To investigate the nature of the turbulence, we may calculate the profiles of broadening for various velocity distributions for the model of 31 Cyg. The best fits seem to be for *isotropic* turbulence. In Figure 7, the dashed line shows the profile for isotropic turbulence giving roughly the line broadening of single supergiants. A Gaussian fits it quite well, as expected for the assumptions in the calculation. The solid curve shows the effect of imposing a $v_{syst} = 10$ km s^{-1} downward velocity on this same turbulence. The profile is still Gaussian at the level of the plot, but it is shifted to the red (3.8 km s^{-1}) and broadened slightly more (ΔFWHM = 1.0 km s^{-1}) by the variable projection of the systematic velocity into the line of sight.

Calculations for *anisotropic* turbulence all give non-Gaussian profiles to some extent. Some of these are shown in Figure 8. Radial turbulence is especially bad in this regard (Figures 8a and 8c) because the strongest emitting regions are near the stellar limb, where the turbulent motions would be mostly perpendicular to the line of sight. Tangential turbulence is considerably better but still decidedly non-Gaussian (Figures 8b and 8d), with enhanced wings not seen in profiles of actual stars (see Carpenter et al. 1991, Figure 3b). Figures 8c and 8d, however, show that *elliptical* anisotropic turbulence, in which one component is much larger than the other, is considerably closer to the observed Gaussian shape, and the departures from the observed Gaussian profiles would be somewhat reduced by convolving the calculated profiles with a Gaussian PSF for a spectrograph, which I have not done. However, these profiles would still have overly broad wings not seen in actual stars. I chose the nature of elliptical turbulence to reflect an isotropic turbulence of 5 km s^{-1} from perhaps thermal motion and 20 km s^{-1} of either radial or tangential macro- or microturbulent motions.

Carpenter & Robinson (1997) and Robinson et al. (1998) have cleverly fit the broadened wings of C II] lines with an anisotropic turbulence somehow averaged over a uniform disk, but that model is clearly inappropriate in light of the large limb effects predicted by ζ Aur binaries (Figure 3). In fact, a calculation with our model, but limited to gas within the limb of the star, gives the awful non-Gaussian profiles seen in Figure 8(e).

Given the distribution of mass in the model and the resulting limb brightening, the Gaussian profiles of intrinsic lines imply a fairly *isotropic* turbulence. They certainly do not allow mostly *radial* turbulence, and they make it unlikely that the turbulence is preponderantly tangential.

4.4. Electron Density and Interpretation of the C II] Multiplet

We have hardly any actual knowledge of the electron densities in the winds/chromospheres of any of these stars. What we do know is how dense the regions emitting the bulk of C II] are. Everything else must somehow come from a *model* calculation.

One of the triumphs of applying physics to cool stars is the use of C II] to derive precise electron densities for a large number of objects. The kinematic analysis of Judge (1994), however, undermines the importance of this result. The redshift he detects in most stars is difficult to reconcile with other aspects of UV analyses, since it requires a $\sim$10 km s^{-1} downdraft of all the emitting gas or something more extreme if only part of the gas is participating. It would be convenient if this redshift were the result of a systematic error in the energy levels, and this may ultimately prove to be the cause of it. The energies of the upper levels of C II] are quoted by Moore (1970) to the nearest 0.1 cm^{-1}, about 1 km s^{-1}, while the wavelengths are somehow known to one more significant figure. Likewise, the enhanced electron densities derived for the red side of these profiles seem to manifest themselves in only one of the line ratios, as though it might be affected by an unrecognized blend, but the dominant 2325.4 Å line would have to be the one affected.

However, if we accept the reality of the shift and enhancement, C II] must be telling us something profound about wind acceleration. C is two orders of magnitude more plentiful than Al, yet lines of the two are roughly the same strength in cool

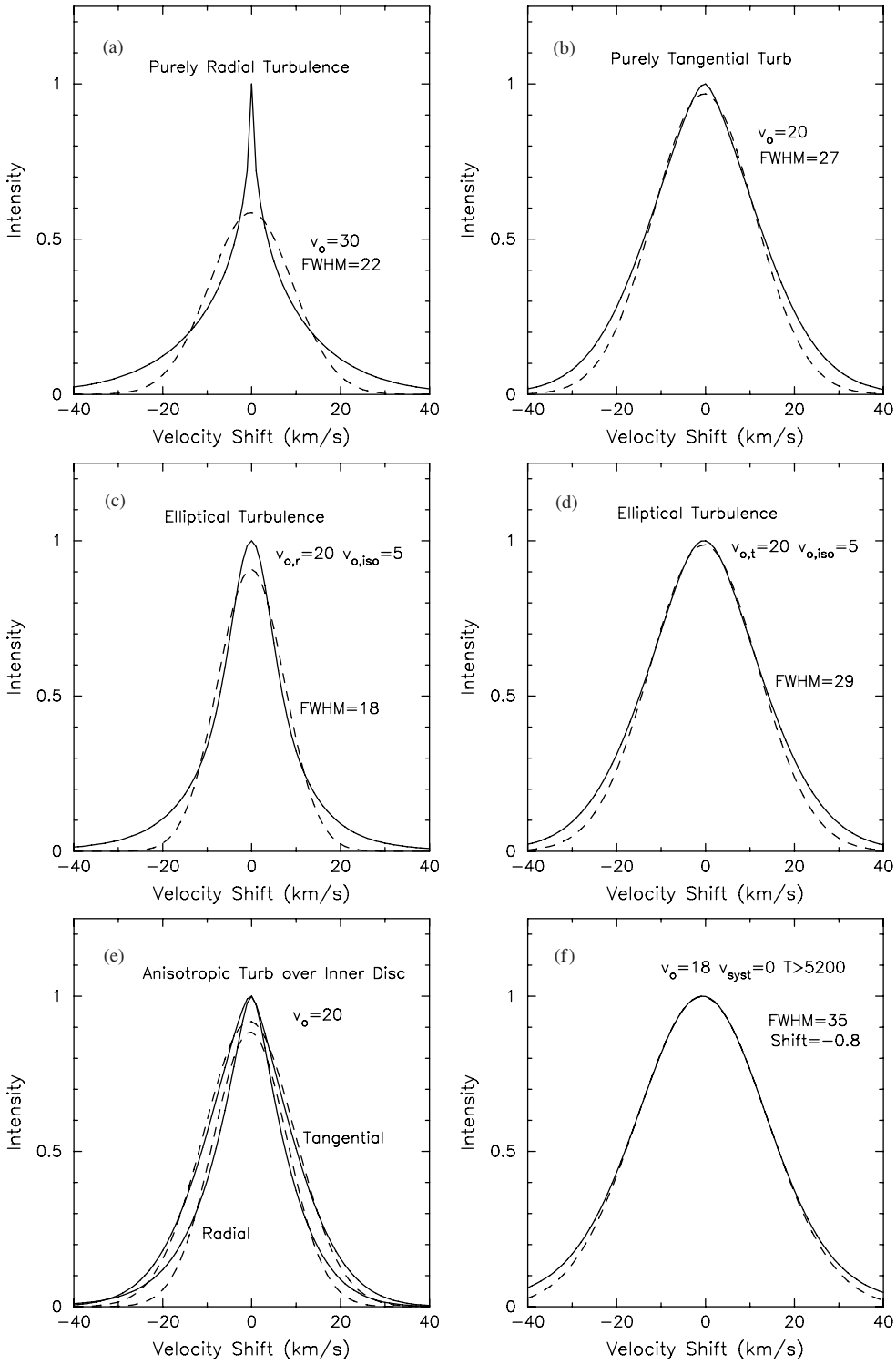

Figure 8. Effects of various types of anisotropic turbulence on calculated line profiles. In these figures, the solid curve is the calculated profile, and the dashed curve is a Gaussian fit. For the more extreme profiles to the left, this Gaussian is fit to the whole profile; for the subtler profiles to the right, the Gaussian is fit to the inner part (Intensity $\geqslant$ 0.5). Panel (a) shows the really awful effect of purely *radial* turbulence, while Panel (b) shows the more subtle effect of purely *tangential* turbulence. Panels (c) and (d) show, respectively, the effect of 20 km s^{-1} of radial or tangential turbulence combined with 5 km s^{-1} of isotropic turbulence. Panel (e) is an experiment with confining radial and tangential turbulence to only the disk. The radial distribution is noticeably different than Panel (a) because most of the emission in Panel (a) comes from *beyond* the edge of the disk. Panel (f) shows the effect of isotropic turbulence with only the gas hotter than 5200 K emitting.

giants. Very little of the C, therefore, may be emitting C II], and it must be produced under rather special conditions to give the observed multiplet ratios of single stars. The broad wings of C II] can be fit by emission in the expanding gas of the upper chromosphere/lower wind with the broadening produced by differential projection of expansion into the line of sight. However, for that approach to work, the inner regions of the chromosphere must be neutral in C, even more so than implied by ionization balance in semi-empirical models such as those of Section 3.2 or measured in 31 Cyg. Figure 8(f) shows such a calculation in which the gas below 5200 K emits no C II]. This calculation gives a reasonable flux, but it does not fit any of

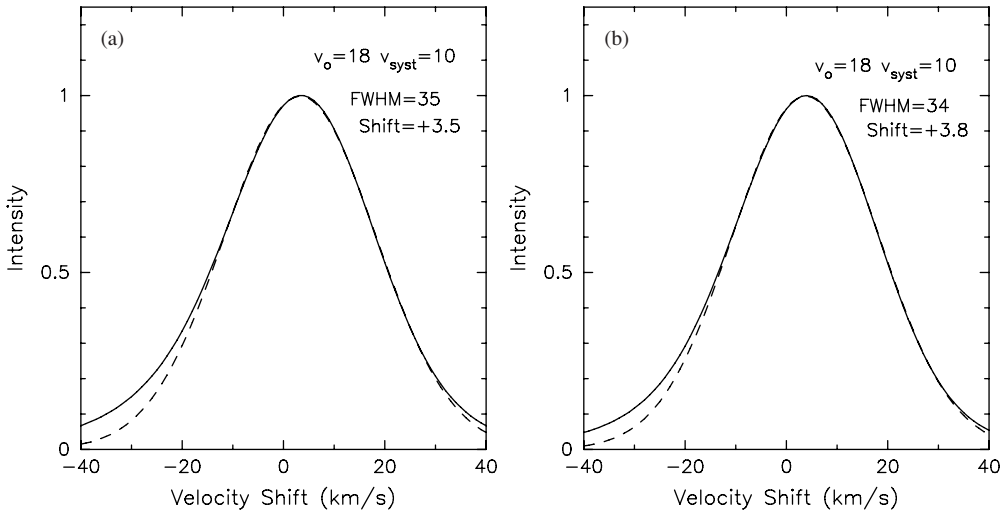

Figure 9. An attempt to fit the peculiar shapes and shifts of C II] emission in windy giants. Calculated profiles are the solid curves; Gaussians fit to the inner parts of these profiles ($I > 0.5$) are dashed curves. In both cases gas in the deeper parts of the chromosphere (cooler than some threshold value) was given a 10 km s^{-1} downward velocity. Panel (a) at left shows the effect of suppressing all the emission at temperatures between 6000 K and 8500 K while letting 30% of the gas below 6000 K emit. Panel (b) at right shows the effect suppressing all emission from gas cooler than 8000 K except for gas with electron densities above $\log(n_e) \geqslant 8.6$. In both cases extra broadening in the wings comes from emission from gas with significant expansion velocity projected into the line of sight.

the other properties of C II]. The average electron density in the emitting gas (5×10^7) is nowhere near the canonical 10^9, *even with the clumping*. The width of the profile is somewhat more than expected for a real star (FWHM = 35 versus 30 km s^{-1} for a weak line like Al II]), the peak is shifted blueward by -0.8 km s^{-1}, and the wings are probably too weak relative to the core. Clearly a more radical departure from the expected ionization/velocity structure is required.

Looking at this more radically, we can get an idea of the conditions required *in the 31 Cyg model* by extending our assumptions about ionization. Given the velocity structure, observationally all the C would be neutral below 7000–8000 K to weight the emission at significant expansion velocity enough to give the extended wings (giving the same sort of effect as the anisotropic turbulence dismissed in Section 4.3), with the bulk of emission coming from locally dense, probably rather cool regions at depth that may have peculiar velocities. Again, this means that C would be *much less ionized* in these atmospheres than predicted by semi-empirical models, with the C II] emission coming from only a moderately small fraction of the gas. However, the similarity of Doppler widths of C II] and other optically-thin lines such as Si II] and Al II] suggests that both are formed in gas with similar turbulence, perhaps in similar parts of the atmosphere. A possible source of the redshift of the line core is preferential excitation in the downward-facing parts of downward-moving elements in the turbulence distribution. This fraction of the gas would have the greatest relative speed with respect to the outward momentum source, and might well be expected to be subjected to the most violent accelerations. Figure 9 shows two experiments in simulating this effect. In Figure 9(a) the emission comes from two sources—all the gas above 8500 K emitting with the velocity structure of Table 2 and 30% of the gas at temperatures below 6000 K emitting with a 10 km s^{-1} downdraft. Figure 9(b) shows the emission for a model in which the gas above 8000 K is emitting with no downdraft and only the cooler gas with $\log(n_e) \geqslant 8.6$ is emitting with a 10 km s^{-1} downdraft. Both calculations give reasonable fluxes and electron densities averaged over the emitting gas (3.5 and 5.5×10^8, respectively) high enough to begin to approximate the observed global values. Thus calculations with the most realistic chromospheric model we can muster are at least *consistent* with Judge's suggestions about C II].

This analysis has necessarily been speculative, although it is much better constrained by actual observations than any alternative analysis, e.g., one based on a traditional semi-empirical model, could have been. I think it is fair to conclude that (1) the broad wings of C II] likely come from formation in the lower wind (the broadening coming from differential expansion), and (2) C may not be ionized in the way expected from the standard non-LTE calculations of semi-empirical atmospheres but may be subject to some other source of ionization associated with the driving mechanism that picks out only part of the radial component of the turbulence distribution. In all these calculations the wings of the C II] line are broadened by formation in gas with significant expansion velocity projected into the line of sight. The asymmetry favoring the blue wing over the red results from having some of the redshifted gas blocked by the star. This effect is seen in actual stars, e.g., α Tau (Carpenter et al. 1991, Figure 3) and γ Cru (Carpenter et al. 1995, Figure 2). Furthermore, as a caveat, we should note (1) that C would be depleted by the first dredge-up (e.g., Luck & Lambert 1985), although this effect is presumably included in my adopted C abundance, and (2) that the observations of ζ Aur binaries do not seem to show mostly neutral C at depth. One should also keep in mind that C II] may eventually destroy a basic assumption of this paper, and practically every other one written about chromospheres and winds of cool giants, that the chromosphere and wind are one continuous structure spread evenly over the face of the star.

4.5. More Highly Ionized Species

The emissions of highly ionized species such as C III] and C IV do not fit readily into our model for 31 Cyg. The level of ionization required is incompatible with the temperatures and densities measured in the outer winds of ζ Aur binaries as well as with the level of ionization actually measured in these winds. However, the *clumping* of the gas throughout the chromosphere/wind gives us ample opportunity to incorporate more highly ionized material deep in the chromosphere and possible ways to excite it. We have assumed that the gas is confined to blobs that fill

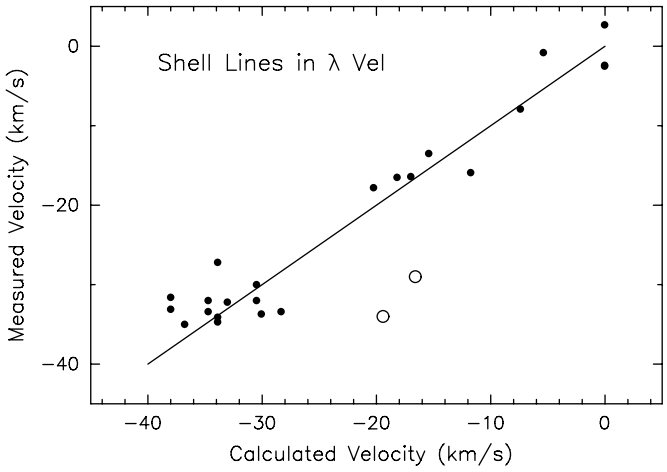

Figure 10. Comparison of shell velocities for λ Vel with calculations for the 31 Cyg model under assumptions about mass loss and ionization. Measured values come from Carpenter et al. (1999, Table 3). The circles are two lines for which the measured values seemed discrepant in Carpenter's paper, one even falling beyond the limits of his Figure 9. Calculated velocities assume $\dot{M} = 9 \times 10^{-9} M_{\odot}$ yr^{-1} and that Fe is doubly ionized at $n_e < 2 \times 10^{6}$.

∼10% of space, surrounded essentially by a vacuum filled with an, as yet unspecified, source of pressure. The energy densities required to drive the wind through gradients of this pressure are certainly sufficiently high to allow higher ionization than the dominant levels we see in the shell lines.

4.6. Velocity Structure from Fe II Self-Reversals

We may use our model for 31 Cyg to test the techniques used to deduce wind structure from shell lines in single stars. The problem here is that such analyses for single stars give winds accelerating much more rapidly than those in ζ Aur binary components. I have used my 31 Cyg model to predict what the velocities of the shell components of strong Fe II lines in λ Vel might be if it had the same velocity structure as 31 Cyg. This is the star with the best evidence for wind acceleration in Fe II self-reversals, for which Carpenter et al. (1991, 1995, 1997, 1999) derived a wind with $\beta = 0.9$, $v_{\infty} = 29$–33 km s^{-1}, and $\dot{M} = 3 \times 10^{-9} M_{\odot}$ yr^{-1}. In this simulation, I calculated the line-center radial optical depth into the atmosphere for the Fe II and Mg II lines measured by Carpenter et al. (1991, 1995, 1997, 1999) and determined the position and expansion velocity for $\tau = 2/3$, as though the intrinsic line emission core comes from the center of the disk. Table 3 gives the results, and Figure 10 displays them. These calculations assume the constraints of Table 2, with turbulence from Column 9. For the mass-loss rate of 31 Cyg, the lines become optically thick very high in the wind, absent ionization of Fe^{+} to Fe^{+2} (Table 3, Column 5), but if we reduce the mass-loss rate somewhat to $9 \times 10^{-9} M_{\odot}$ yr^{-1}, to partially reflect Carpenter's lower value, and allow for ionization of Fe to Fe^{+2} for $n_e < 2 \times 10^{6}$ (Table 2, Column 8), we get velocities in much better agreement with observed values, as seen in Figure 10. Unfortunately we cannot apply this sort of analysis directly to the self-reversals of Fe II lines in 31 Cyg because the emission is formed not in the inner chromosphere, as in single stars, but by scattering light from the B star in a huge shell surrounding the binary system.

These results show that we can actually reproduce the sort of observations taken to indicate a rapid acceleration of the chromosphere in a single star with a model accelerating much more slowly. The secret for doing this is the realization that the observed absorption is limited by ionization of the outer wind as discussed in Section 4.2. Therefore, there is really no compelling reason to believe the wind acceleration in the single windy giants is necessarily any faster than in binary components.

There is evidence in occultations, as well as in the Hα profiles, that the chromospheres/winds of single stars are much more extended than commonly thought. An occultation in Hα emission for the single M supergiant 119 Tau at M2 Ib (White et al. 1982) and an image of α Ori at M2 Iab (Hebden et al. 1987) both showed Hα emission, hence significant optical depths in the Lyman lines, out to at least twice the photospheric radii. Also, all of these cool supergiants show asymmetric Hα profiles, indicating that the line core is formed in the wind at least some of the time (Mallik 1993). Furthermore, in their model of the wind of α Ori, Harper et al. (2001) find a velocity/density structure giving even slower acceleration than we find in 31 Cyg or they found (Harper et al. 2005) in ζ Aur.

Table 3
Calculated Expansion Velocties for Shell Lines

Multiplet	λ (Å)	log(LSF) at 6000 K	$v^{obs}_{\lambda Vel}$ (km s^{-1})	v^{calc}_{31Cyg} (km s^{-1})	$v^{calc}_{\lambda Vel}$ (km s^{-1})
Fe II UV1	2599.40	0.86	−35.0	−83.4	−38.0
Mg II UV1	2795.52	0.66	−31.6	−83.8	−38.0
Mg II UV1	2802.70	0.36	−33.1	−83.7	−38.0
Fe II UV1	2598.37	0.35	−33.4	−82.4	−34.7
Fe II UV1	2585.88	0.30	−34.7	−82.2	−33.9
Fe II UV1	2607.09	0.25	−34.1	−82.0	−33.9
Fe II UV3	2332.80	0.19	−32.2	−81.8	−33.0
Fe II UV62	2755.73	0.04	−32.0	−81.0	−34.7
Fe II UV3	2364.83	−0.01	−30.0	−80.6	−30.5
Fe II UV1	2625.66	−0.05	−33.7	−80.3	−30.1
Fe II UV32	2739.55	−0.05	−27.2	−80.3	−33.9
Fe II UV3	2338.01	−0.06	−32.0	−80.3	−30.5
Fe II UV1	2617.62	−0.16	−33.4	−79.4	−28.4
Fe II UV35	2362.02	−0.62	−17.8	−69.8	−20.3
Fe II UV35	2331.30	−0.75	−29.0	−64.0	−16.6
Fe II UV35	2366.59	−0.84	−13.5	−64.0	−15.4
Fe II UV64	2593.72	−0.91	−34.0	−59.2	−19.4
Fe II UV64	2591.52	−0.93	−16.5	−53.9	−18.2
Fe II UV32	2736.97	−0.99	−16.4	−50.1	−17.0
Fe II UV35	2354.89	−0.99	−15.9	−49.8	−11.8
Fe II UV63	2761.81	−1.37	−7.9	−25.8	−7.4
Fe II UV63	2772.72	−1.48	(−0.8)	−19.8	−5.4
Fe II UV260	2741.40	−2.86	(−2.5)	−0.5	0.0
Fe II UV32	2732.41	−3.11	+2.7	−0.2	0.0
Fe II UV32	2759.34	−3.18	(−2.4)	−0.1	0.0

5. DISCUSSION

The importance of ζ Aur binaries is that they tell us just where the bulk of the gas is in the inner few stellar radii of the stars' chromospheres or winds. We can measure column densities directly, and get at least a reasonable idea of how dense and hot it is throughout this critical zone where most of the energy is injected into a star's wind. Furthermore, with models such as those of Section 3.2, we know that this gas must be emitting the intrinsic lines that we would easily see absent the B companions. The structure is, therefore, constrained in ways it simply cannot be in any analysis of a single star. I have subjected the model for 31 Cyg, and by extension models for other ζ Aur binaries, to tests based on various sorts of emission from their chromospheres/winds. That such a model reproduces the intrinsic C II], Al II], and thermal radio emission to ∼50% with a minimum of fiddling is an excellent test of the reality of the

structure derived. Furthermore, the clumping inferred for such models provides an excellent opportunity (note that this really is fiddling) to accommodate tenuous material emitting lines of the more highly ionized species. This agreement is reassuring, inasmuch as most of the properties of the model are constrained by *observations*. The chief uncertainties involve ionization of H throughout the atmosphere, which is *not* measured well observationally, and ionization of H and the metals in the outer wind ($T_e > 9000$ K) where many of the self-reversals of strong lines would probably be formed.

5.1. Alfven-Wave Models

There are several fairly extensive classical investigations of the conditions required for driving winds by Alfven waves that provide potentially testable predictions (Hartmann & McGregor 1980; Hartmann & Avrett 1981; Holzen et al. 1983; Kuin & Ahmad 1989). For the most part these suffer from limitations of assuming that the gas is effectively coupled to the fields (i.e., fully ionized), from not exploring the mechanisms of transfer of momentum from wave to gas realistically (although Holzer et al. did begin this process), and therefore from relying on somewhat nonphysical theories of how the waves are damped. Suzuki (2007) has more recently calculated more realistic Alfven models driving wind through flux tubes diverging from the surface of the star between closed structures. This rather Sun-like geometry seems to be required to explain the chromospheric hybrid stars. In these models the wind seems to accelerate from the star much farther above the surface than observed in ζ Aur binaries or inferred in single stars, and the mean temperatures reached in the winds also seem much higher than observed.

There are a couple of ways of applying a wave model for driving a wind. In the more fundamental approach, one would use theories of how such waves are generated and how they interact with partially ionized media to predict the structure and properties of winds theoretically. Holzer et al. (1983, Section VI) actually calculated some models of this sort. Unfortunately, the theories required to do that are difficult to apply, and knowledge of magnetic fields of actual stars that would support such waves is lacking. The alternative is to form a semi-empirical model for wave-driven winds, somewhat like the chromospheric models I have been discussing, and determine what the properties it must have to fit the observed structure of a wind (namely, mass-loss rate, terminal velocity, velocity–density structure). A good example of this second approach is the analyses of ζ Aur binaries by Kuin & Ahmad (1989). Their models find that damping of the wave amplitude must decrease with height to fit observed velocity profiles, as one might well expect theoretically to keep the terminal velocity consistent with observation. Their models also give predictions of the level of turbulence in the chromosphere/wind by associating the lateral displacements of gas by such waves with the observed Doppler widths of gas in the atmospheres of these stars. Predicted Doppler widths, both by Kuin & Ahmad and Hartmann & Avrett (1981) seem to be larger than the observed turbulence, both in shell absorptions in ζ Aur binaries and in the optically-thin emission lines of single windy giants. Furthermore, since Alfven waves are transverse, the "turbulence" would be anisotropic to first order. This prediction is at odds with the observation of isotropic turbulence, although it is based on the idealization of radial magnetic fields, while the actual topology might well be more complicated (see Cassinelli et al. 1995).

Kuin & Ahmad (1989) found from their semi-empirical models that the damping length for Alfven waves must increase with height. The most convincing mechanism for transferring energy from the wave to the gas, i.e., damping it, is ion-neutral friction in which there is a phase lag between the wave's transferring momentum to ions and the ions' subsequently transferring it to neutrals. Hartmann & McGregor (1980) discussed this mechanism, although they had no way of applying it *a priori*. For waves with long periods, the transfer can be so rapid that the neutrals are effectively bound to the ions through elastic collisions, and there is little dissipation of wave energy or transfer of momentum. For high frequency, on the other hand, the neutrals cannot respond fast enough to the passage of a wave to partake in its displacements, and the ions just stir them up and dissipate wave motion as heat. Since the dissipated wave energy would go primarily into heating, this mechanism would be better for heating the chromosphere/wind than driving its outflow. Most of the wave energy would be available for heating the wind but not for driving it, since the measured temperatures in these winds are much too low to drive them by thermal expansion (see Section 3). Presumably the *momentum* of the wave would be transferred into wind motion. However, since the ratio of energy to momentum (E/p) goes as $1/v$, with the Alfven speed generally larger than either a thermal or turbulent velocity, philosophically an attractive driving mechanism would transfer its energy to heat or some other mass motion as an intermediate stage. This is why it is so hard to drive winds with radiation pressure ($E/p \sim 1/c$). If all the waves had the same frequency, we would expect the momentum to be deposited in a narrow range of density, hence height, contrary to measurements of the acceleration of actual winds.

The mechanism of ion-neutral friction would imply a damping length that decreased with height contrary to Kuin & Ahmad's (1989) result. However, it also implies that waves of different frequencies would be absorbed at different height and, therefore, that the *spectrum* of Alfven waves would determine the velocity profile of the wind. At this point our knowledge of the photospheric motions that might be exciting Alfven waves and the spectrum they would produce seems too sketchy to make any testable predictions about a wind's velocity structure.

5.2. An Alternative Wind Mechanism

Let us now take the liberty to speculate about a different way of driving the mass loss of these windy giants. We have developed here a picture of what conditions are required to drive the wind of one particularly well observed wind structure. Pressures required are an order of magnitude greater than those of the implied density/temperature structure. That the microturbulence required to fit line shapes and widths seems to be rather isotropic means that we likely are not simply seeing the effects of globally organized Alfven waves passing through the gas, as proposed by Hartmann & McGregor (1980) and implied by the models of Airapetian et al. (2000), for example. There may be another way of supporting a wind with magnetic fields, namely using *chaotic fields* emerging from the star and diffusing through the gas into space to drag the gas along with it and away from the star. Some form of this idea was implicit in our previous musings about the wind structure of 31 Cyg (Eaton & Bell 1994, Section 6), and Mullan et al. (1998) may have waved at it in passing. This very speculative picture is fundamentally different from the Alfven model in that the magnetic field being lost can constitute a moderate amount of luminosity. In the standard Alfven model, gas is driven approximately radially from the star along magnetic flux lines anchored permanently in the stellar surface. Here, magnetic flux would be lost at approximately

the same rate as the gas and constitute a significant component of the energy loss in the wind through its adiabatic expansion. Such a chaotic field would give a much more isotropic pressure, which would impress itself on the random velocities of the gas. We may estimate the effect by assuming the pressures driving the wind are in equipartition with the kinetic energy of random motions (turbulence) in the gas. For this condition the driving energy is $\frac{1}{2}NkT$ per degree of freedom (three of them), N being the number of particles in a random blob of mass M. The kinetic energy of the blob is $\frac{1}{2}Mv_{\rm equ}^2$ (per degree of freedom), so that equipartition gives $Mv_{\rm equ}^2 = NkT$, or

$$v_{\rm equ} = (k/\langle m\rangle)^{0.5} T_{\rm therm}^{0.5} = 0.08 T_{\rm therm}^{0.5} \quad (6)$$

where we have taken the average mass per particle to be $1.3m_{\rm H}$. This is to within a factor of $\sqrt{\gamma}$ of the sound velocity, but for our elevated artificial temperature, $T_{\rm therm}$. For values of the driving temperature, $T_{\rm therm}$ (Column 4 of Table 2), we get the turbulent velocities given in Column 9 of Table 2. These values are comparable to the line-of-sight random velocities measured in cool (super)giants, and this fact argues that the driving force must be able to produce the random motions observed. It is unlikely, therefore, to be global Alfven waves. Of course, the pressure of these turbulent motions is itself a major source of momentum and energy in extending the atmosphere and driving the wind.

Energy input determines the magnetic fields required in this model, since the magnetic energy density must be greater than the energy per unit volume required to lift the mass out of the potential of the star, $B^2/8\pi > GM_{\rm K}\rho/R_*$. For our model, this leads to a field strength of 25 Gauss. If we assume the energy loss is double the potential energy from kinetic energy of the wind and emission from it, the field strength increases only to 35 Gauss.

Such magnetic fields are compatible with measured fields in AGB supergiants and Mira variables, the only ones for which field strengths can be detected reliably. Masers excited in clumps in such stars' winds reveal magnetic fields through Zeeman splitting (e.g., Vlemmings et al. 2002; 2005a, 2005b). Various molecules (OH, H_2O, SiO) form maser emission at different distances from a star, i.e., at different densities, and the field strength deduced from them shows a gradient with height, as expected. Extrapolation of these fields to the surface gives values of order 10^2 G for the Miras and 10^3 G for the supergiants (Vlemmings et al. 2002). These would be plenty strong enough for driving winds either by our speculative model or by Alfven waves. There is some indication of a global structure of the fields (Richards et al. 2004), which would probably favor Alfven waves. However, inasmuch as it is generally thought that the winds in these very cool stars are driven by radiation pressure on grains (Lamers & Cassinelli 1999, Chapter 7), possibly excited by pulsation (Willson 2007), it is not clear what these measurements of magnetic fields in AGB stars mean for the winds of the hotter stars. Suffice it to say, that if these highly evolved stars, which might be expected to have lost most of their initial rotational energy, are so highly magnetic, then less evolved ones such as G–K giants and supergiants must be magnetic too.

This kind of driving has the advantage over Alfven waves of being able to begin to explain the variation of mass loss from star to star in a way related to stellar structure and evolution. In our simulation of driving with thermal profile, the expansion–velocity structure is determined by the temperature (i.e., energy–density) profile, while the mass-loss rate is arbitrary, determined by supplying enough energy at some $\dot{M}$ to maintain the energy–density profile. With magnetic-flux emergence as the driving mechanism, the magnetic energy corresponds to the infusion of thermal energy in the coronal model; mass-loss rate, therefore, is proportional to the rate at which the magnetic field emerges. This is very attractive in that there are indications that the winds of the giants vary in response to changes that can re-excite dynamos in their cores. See Mullan & MacDonald (2003) for changes of mundane giants, and recall the shells episodically thrown off by pulsing AGB stars. Alfven waves would most likely be excited by convection, therefore be proportional to luminosity, and be little affected by the strength of the passive magnetic fields serving as their medium.

As an alternative to chaotic magnetic fields filling the voids in chromospheric gas, we may imagine Alfven waves trapped in the cavities between ionized blobs. These waves would have speeds approaching the speed of light as the density dropped, and would be reflected off the blobs if their frequencies were below the cyclotron frequency. The critical frequency would rise as the material became more highly compressed (denser). Eaton & Bell (1994) actually had this mechanism in mind as the driving pressure in such atmospheres. There must be a rich optics of these Alfven waves waiting to be discovered.

6. SUMMARY

I have constructed a model for the chromosphere and wind of 31 Cyg which is based on measurements of physical properties in the outer atmospheres of 31 Cug and other classical ζ Aur binaries. It goes beyond other such models in that it derives the poorly understood turbulence and clumping of the gas from the pressures driving the wind's expansion. It predicts emission of optically-thin lines and microwave continuum to within 50% of observed values, excellent agreement in the circumstances. In this model, the momentum flux required to drive the wind determines the stratification of the chromosphere where intrinsic lines would be formed. That momentum flux gives much lower densities than the stratification from thermal momentum flux alone, with the consequence that the gas must be clumped to produce the observed flux in intrinsic lines. We also find that this model can reproduce most of the properties of single stars' chromospheric spectra and argue that the evidence for fundamental differences between single stars and these binary components is rather weak.

We must keep in mind, however, that there are inconsistencies in this picture. The ionization of C, for instance, is a problem. It cannot be mostly singly ionized, as it seems to be observationally, without giving fluxes much larger than observed, and the model for 31 Cyg does not predict the redshifts seen in single supergiants. C II] multiplet ratios from the model likewise would not predict the large global electron densities found from C II] in single stars. However, there are also inconsistencies in the interpretation of C II] in the single stars themselves, as I discuss in Section 4.4.

The biggest fundamental uncertainty in all analyses of cool giants' winds, implicit in Suzuki's (2007) models, is whether the wind and chromosphere are a single unit, as we assume here, or broken up into regions bound to the star by magnetic loops and a wind that flows around them, as in the Sun. This is probably the biggest outstanding question about the outer atmospheres of all the cool giants and supergiants. However, we may be able to address this question seriously in the near future. Interferometers should begin resolving the

disks of these cool supergiants, actually making it possible to see their limb darkening and surface granulation and to map out their chromospheres directly. Such images will give important tests related to chromospheric structure by determining how extended and uniform these structures really are. Thirty-one Cyg should have an angular diameter near 3.9 mas. The Palomar Testbed Interferometer, for instance, has already resolved stellar shells at the milliarcsecond level (Lane et al. 2006), and new developments are expected to give a resolution near 0.3 mas (M. Muterspaugh 2008, private communication). This resolution corresponds to more than 10 picture elements across even the relatively small visible disk of 31 Cyg. Larger stars will give even more detail.

I dedicate this paper to John S. Mathis who seemed to have the visceral intuitive grasp of physics required to address the sort of problems I have discussed in this paper. If I had had the sense to take his advice to work in this area when I was in graduate school, I probably would have written it years ago. A referee made several useful suggestions for improving this paper. This research has been supported by the NSF through grant HRD-9706268 and by NASA through grant NCC5-511 to Tennessee State University.

REFERENCES

Ahmad, I. A., & Stencel, R. E. 1988, ApJ, 329, 797
Airapetian, V. S., Ofman, L., Robinson, R. D., Carpenter, K., & Davila, J. 2000, ApJ, 528, 965
Allen, C. W. 1973, Astrophysical Quantities (3rd. ed; London: Athlone)
Avrett, E. H., & Loeser, R. 1992, in ASP Conf. Ser. 26, Seventh Cambridge Workshop on Cool Stars, Stellar Systems, and the Sun, ed. M. S. Giampapa & J. A. Bookbinder (San Francisco, CA: ASP), 489
Baade, R., Kirsch, T., Reimers, D., Toussaint, F., Bennett, P. D., Brown, A., & Harper, G. M. 1996, ApJ, 466, 979
Basri, G. S., Linsky, J. L., & Eriksson, K. 1981, ApJ, 251, 162
Bauer, W. H., & Stencel, R. E. 1989, ApJS, 69, 667
Blum, R. D., & Pradhan, A. K. 1992, ApJS, 80, 425
Carpenter, K. G., & Robinson, R. D. 1997, ApJ, 479, 970
Carpenter, K. G., Robinson, R. D., Harper, G. M., Bennett, P. D., Brown, A., & Mullan, D. J. 1999, ApJ, 521, 382
Carpenter, K. G., Robinson, R. D., & Judge, P. G. 1995, ApJ, 444, 424
Carpenter, K. G., Robinson, R. D., Wahlgren, G. M., Ake, T. B., Ebbets, D. C., & Walter, F. M. 1991, ApJ, 377, L48
Cassinelli, J. P., & Hummer, D. G. 1971, MNRAS, 153, 9
Cassinelli, J. P., Ignace, A., & Bjorkman, J. E. 1995, in IAU Symp. 163, Wolf-Rayet Stars: Binaries, Colliding Winds, Evolution, ed. K. A. van der Hucht & P. M. Williams (Dordrecht: Kluwer), 191
Drake, S. A., Brown, A., & Reimers, D. 1987, in 5th Cambridge Workshop on Cool Stars, Stellar Systems, and the Sun, ed. J. L. Linsky & R. E. Stencel (Berlin: Springer)
Drake, S. A., & Linsky, J. L. 1986, AJ, 91, 602
Eaton, J. A. 1992, MNRAS, 258, 473
Eaton, J. A. 1993a, ApJ, 404, 305
Eaton, J. A. 1993b, AJ, 105, 1525
Eaton, J. A. 1993c, AJ, 106, 2081
Eaton, J. A. 1994, AJ, 107, 729
Eaton, J. A. 1995, AJ, 109, 1797
Eaton, J. A. 1996, in ASP Conf. Ser. 109, 9th Cambridge Workshop on Cool Stars, Stellar Systems, and the Sun, ed. R. Pallavicini & A. K. Dupree (San Francisco, CA: ASP)
Eaton, J. A., & Bell, C. 1994, AJ, 108, 2276
Eaton, J. A., & Henry, G. W. 1996, in IAU Symp. 176, Stellar Surface Structure, ed. K. G. Strassmeier & J. L. Linsky (Dordrecht: Reidel), 415
Hartmann, L., & Avrett, E. 1981, SAO Spec. Rept., 392, 197
Hartmann, L. W., & McGregor, K. B. 1980, ApJ, 242, 260
Haisch, B. M., Linsky, J. L., Weinstein, A., & Shine, R. A. 1977, ApJ, 214, 785
Harper, G. M. 1990, MNRAS, 243, 381
Harper, G. M. 1992, MNRAS, 256, 37
Harper, G. M. 1996, in ASP Conf. Ser. 109, 9th Cambridge Workshop on Cool Stars, Stellar Systems, and the Sun, ed. R. Pallavicini & A. K. Dupree (San Francisco, CA: ASP)
Harper, G. M., Brown, A., Bennett, P. D., Baade, R., Walder, R., & Hummel, C. A. 2005, AJ, 129, 1018
Harper, G. M., Brown, A., & Lim, J. 2001, ApJ, 551, 1073
Hebden, J. C., Eckart, A., & Hege, E. K. 1987, ApJ, 314, 690
Holzer, T. E., Flå, T., & Leer, E. 1983, ApJ, 275, 808
Johnson, H. R., & Klinglesmith, D. A. 1965, in Proc. 2nd Harvard-Smithsonian Conf. on Stellar Atmospheres, ed. E. H. Avrett, O. J. Gingerich, & C. A. Whitney, SAO Spec. Rept. No., 167, 221
Judge, P. G. 1986a, Application to Arcturus (α Boo K2 III), MNRAS, 221, 119
Judge, P. G. 1986b, to α Tau (K5 III) and β Gru (M5 III), MNRAS, 223, 239
Judge, P. G. 1988, in IAU Symp. 132, The Impact of Very High S/N Spectroscopy on Stellar Physics, ed. G. Cayrel de Strobel & M. Spite (Dordrecht: Kluwer), 163
Judge, P. G. 1990, ApJ, 348, 279
Judge, P. G. 1992, in ASP Conf. Ser. 26, 7th Cambridge Workshop on Cool Stars, Stellar Systems, and the Sun, ed. M. S. Giampapa & J. A. Bookbinder (San Francisco, CA: ASP), 403
Judge, P. G. 1994, in the Chromosphere of α Tauri, ApJ,, 430, 351
Judge, P. G., & Carpenter, K. G. 1998, ApJ, 494, 828
Judge, P. G., & Jordan, C. 1991, ApJS, 77, 75
Judge, P. G., Jordan, C., & Feldman, U. 1992, ApJ, 384, 613
Kelch, W. L., Chang, S.-H., Furenlid, I., Linsky, J. L., Basri, G. S., Chiu, H.-Y., & Maran, S. P. 1978, ApJ, 220, 962
Kuin, N. P. M., & Ahmad, I. A. 1989, ApJ, 344, 856
Lamers, H. J. G. L. M., & Cassinelli, J. P. 1999, Introduction to Stellar Winds (Cambridge: Cambridge Univ. Press)
Landsman, W., & Simon, T. 1993, ApJ, 408, 305
Lane, B. F., Retter, A., Eisner, J. A., Thompson, R. R., & Muterspaugh, M. W. 2006, in Proc. SPIE 6268, Advances in Stellar Interferometry, ed. J. D. Monnier, M. Schller, & W. C. Danchi (Bellingham, WA: SPIE), 50
Luck, R. E., & Lambert, D. L. 1985, ApJ, 298, 782
Mallik, S. V. 1993, ApJ, 402, 303
McMurray, A. D. 1999, MNRAS, 302, 37
McMurray, A. D., & Jordan, C. 2000, MNRAS, 313, 423
McMurray, A. D., Jordan, C., & Carpenter, K. G. 1999, MNRAS, 302, 48
Milkey, R. W., Ayres, T. R., & Shine, R. A. 1975, ApJ, 197, 143
Moore, C. E. 1970, NSRDS-NBS 3, Section 3
Mullan, D. J., Carpenter, K. G., & Robinson, R. D. 1998, ApJ, 495, 927
Mullan, D. J., & MacDonald, J. 2003, ApJ, 591, 1203
Osterbrock, D. E. 1974, Astrophysics of Gaseous Nebulae (San Francisco, CA: Freeman)
Richards, A. M. S., et al. 2004, in Proc. 7th Symp. of the European VLBI Network on New Developments in VLBI Science and Technology, ed. R. Bachiller, F. Colomer, J.-F. Desmurs, & P. de Vicente (Obs. Astr. Nac. Spain), 209
Robinson, R. D., Carpenter, K. G., & Brown, A. 1998, ApJ, 503, 396
Schröder, K.-P., Reimers, D., Carpenter, K. G., & Brown, A. 1988, A critical test using ζ Aurigae-type K supergiants, A&A,, 202, 136
Stencel, R. F., Linsky, J. L., Brown, A., Jordan, C., Carpenter, K. G., Wing, R. F., & Czyzak, S. 1981, MNRAS, 196, 47
Stencel, R. E., Linsky, J. L., Mullan, D. J., Basri, G. S., & Worden, S. P. 1980, ApJS, 44, 383
Suzuki, T. K. 2007, ApJ, 659, 1592
Tayal, S. S., Burke, P. G., & Kingston, A. E. 1984, J. Phys. B: At. Mol. Phys., 17, 3847
Vernazza, J. A., Avrett, E. H., & Loeser, R. 1973, ApJ, 184, 605
Vlemmings, W. H. T., Diamond, P. J., & van Langevelde, H. J. 2002, A&A, 394, 589
Vlemmings, W. H. T., van Langevelde, H. J., & Diamond, P. J. 2005a, A&A, 434, 1029
Vlemmings, W. H. T., van Langevelde, H. J., & Diamond, P. J. 2005b, Mem. Soc. Astron. Ital., 76, 462
Wareing, C. J., Zijlstra, A. A., & O'Brien, T. J. 2007, ApJ, 660, L129
White, N. M., Kreidel, T. J., & Goldberg, L. 1982, ApJ, 254, 670
Willson, L. A. 2007, in ASP Conf. Ser. 378, Why Galaxies Care About AGB Stars: Their Importance as Actors and Probes, ed. F. Kerschbaum, C. Charbonnel, & R. F. Wing (San Francisco, CA: ASP), 211
Wilson, O. C., & Abt, H. A. 1954, ApJS, 1, 1
Wright, K. O. 1959, Publ. Dominion Astrophys. Obs. Victoria, 11, 77
Wright, K. O. 1970, Vistas Astron., 12, 147
Zarro, D. M., & Rodgers, A. W. 1983, ApJS, 53, 815